

# Fatigue resistant design

## How to improve fatigue life?

### In order of importance

- Nucleation inhibition
- Crack growth inhibition

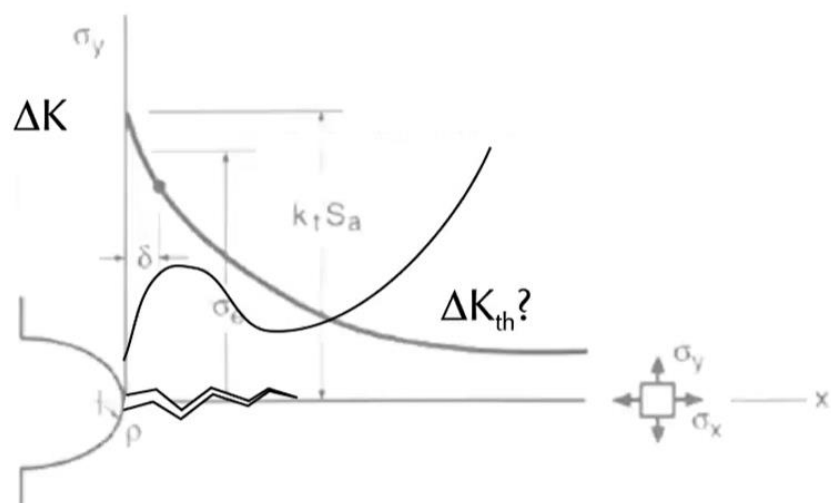
### Inhibiting crack nucleation

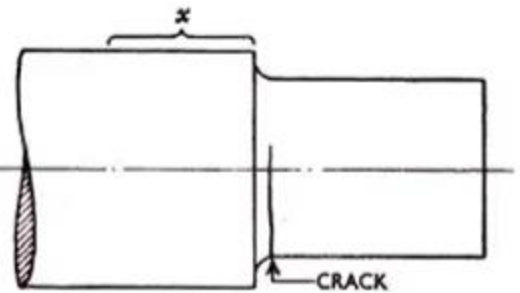
Remove notches and stress concentrations

Remove internal material discontinuities

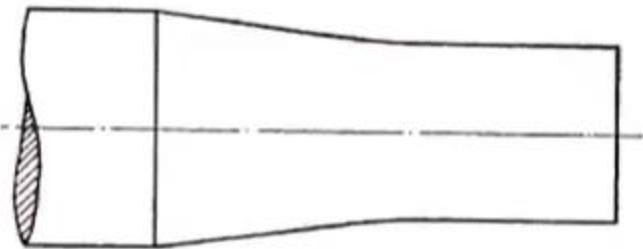
Surface treatment

### Weld seam location and design

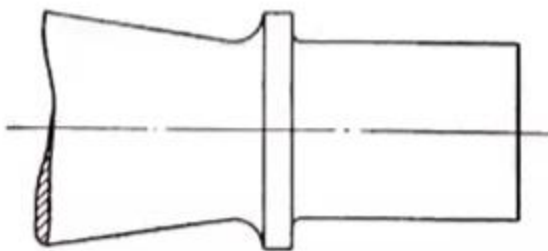




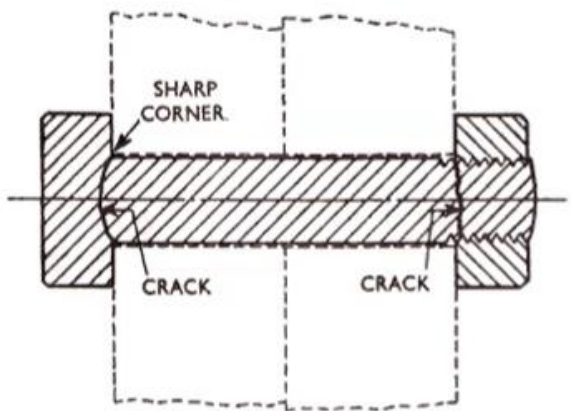
*a* With a parallel portion.



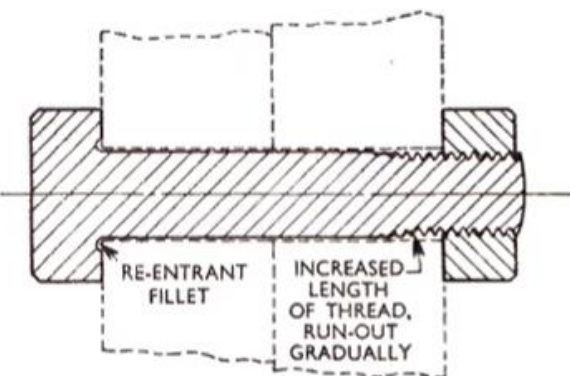
*b* Tapered.



*c* Tapered and with shoulder.



*a* Usual locations of cracks.



*b* Improved type of bolt.

**Figure 10.26** Usual location (a) of fatigue cracks in a bolt and (b) some measures to improve fatigue resistance. (From [Cottell 56]; reprinted by permission of the Council of the Institution of Mechanical Engineers, London, UK.)

# Surface treatment

Hardening

Shot peening

Polishing

## Retarding crack growth

Damage-tolerant –design, with crack arresters

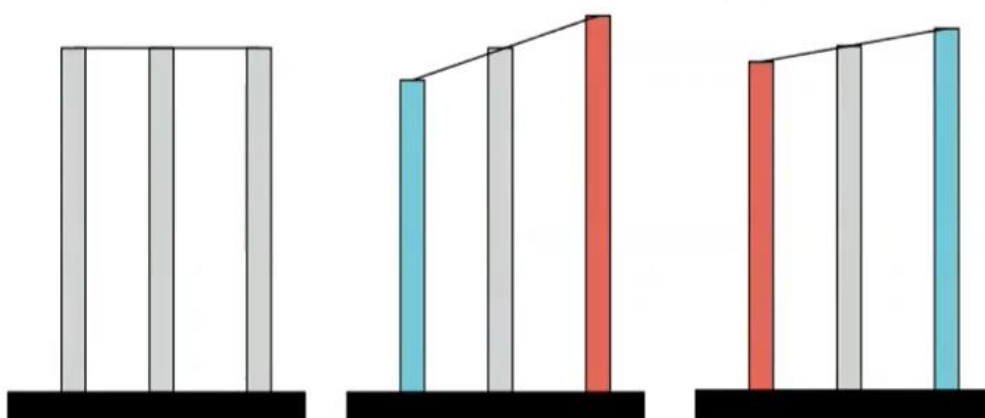
## Residual stresses

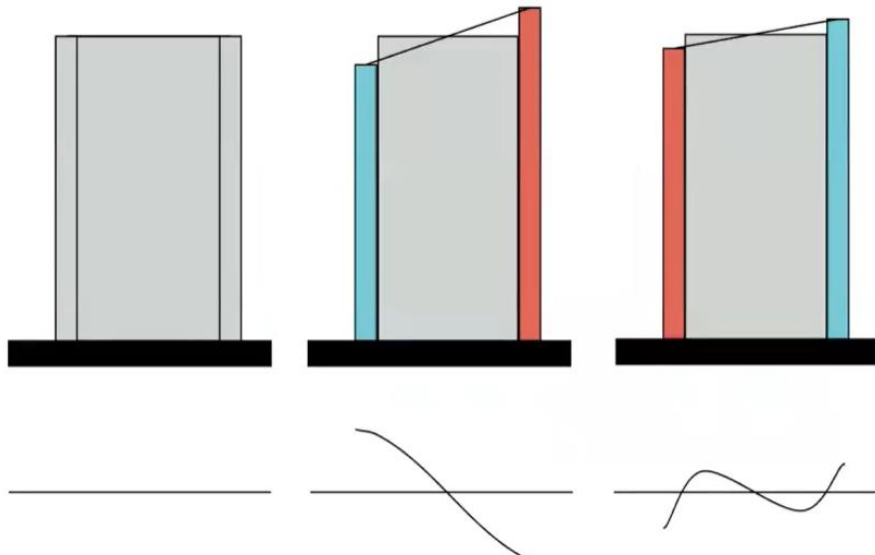
### Stresses that were left behind

- Uneven plastic deformation
- Uneven material properties

#### Strains must be continuous and compatible

- Stresses mediate, when necessary





## Residual stresses

Often from manufacturing (welding, thermal treatment jne.)

Can be used to our advantage (e.g. shot peening)

Often detrimental to

- Fatigue endurance
- Stress corrosion cracking resistance

Common "scapegoat"

## Can be measured

**Non-destructively**

- X-ray -diffraction
- Barkhausen

**Slightly destructively**

- Hole drilling

**Destructively**

- Contour etc.

# Environmentally assisted cracking – EAC

## Environmentally assisted cracking

**Generic term for phenomena, where environment significantly contributes to fracture**

**Several mechanisms**

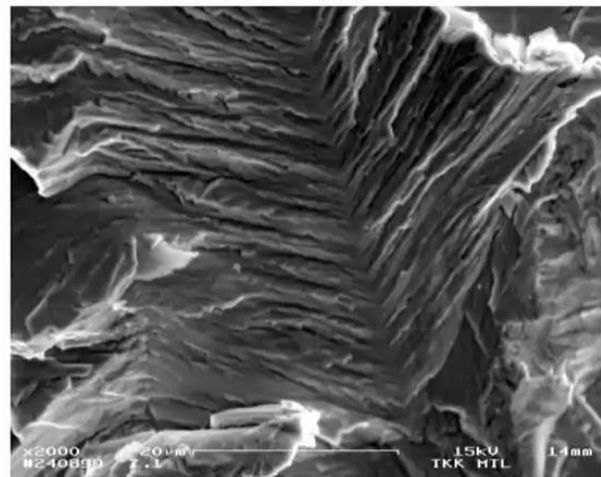
**Here:**

- Stress corrosion cracking (SCC)
- Hydrogen attack
- Hydrogen embrittlement

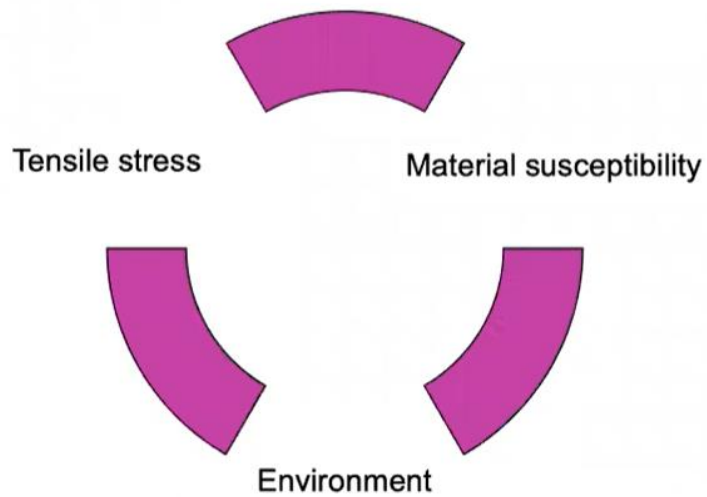
## Stress corrosion

### Stress corrosion

- Brittle-like fracture (no plastic deformation)
- Gradual degradation
- Crack growth at small (global) stresses
- Mode I crack growth
  - IGSCC
  - TGSCC



**Stress corrosion becomes possible,  
when:**

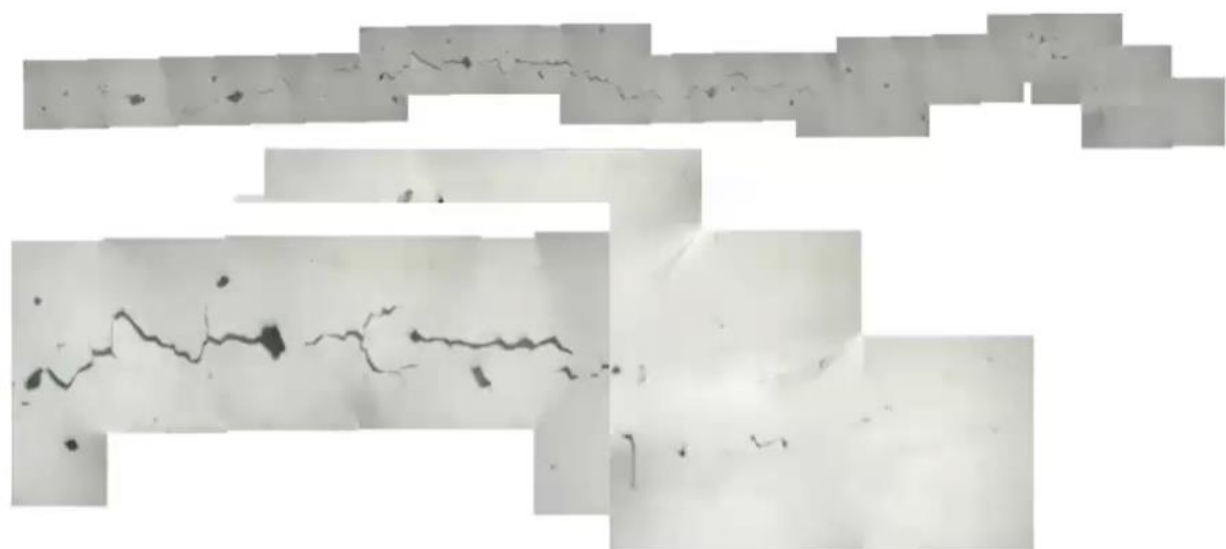


**Stress corrosion cracking**





Photo 5. Typical transgranular, branched crack pattern of chloride SCC in austenitic stainless steel.



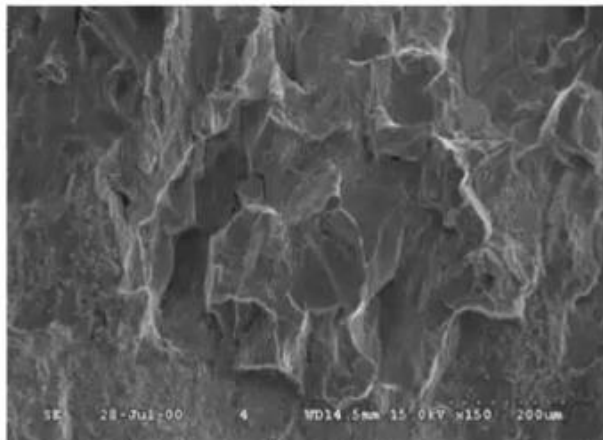


Figure 3 Fracture surface of 304L warm-rolled to 739MPa YS tested in simulated BWR water at 288°C

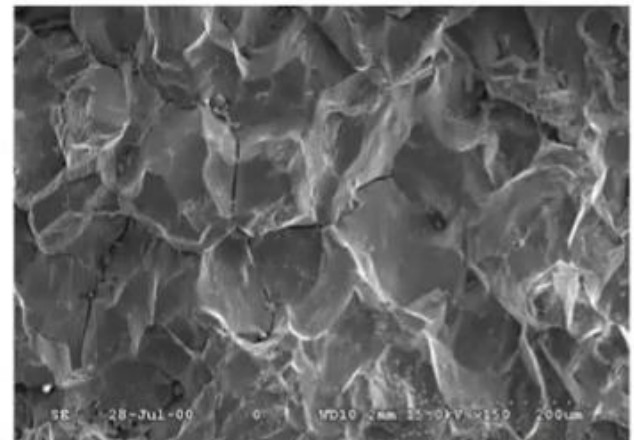


Figure 4 Fracture surface of 304L cold-rolled to 719MPa YS in simulated BWR water at 288°C.

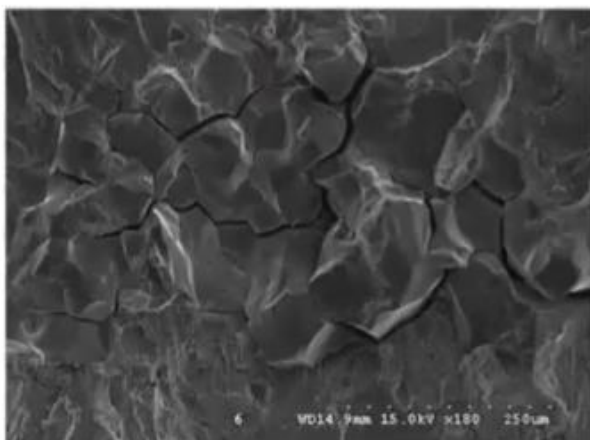


Figure 5 Fracture surface of 316L WR to 568MPa YS in simulated BWR water at 288°C

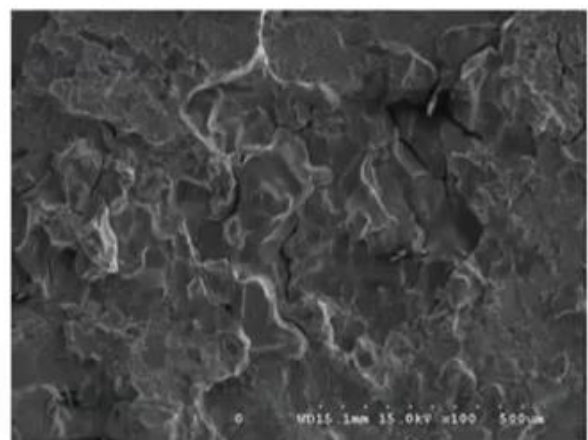
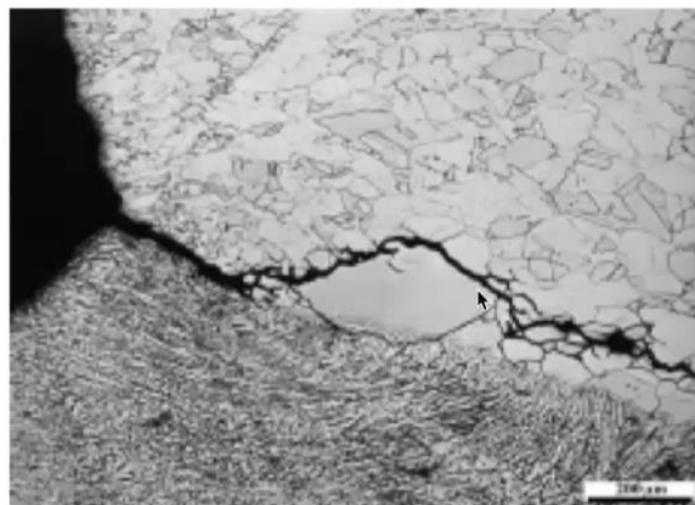


Figure 6 Fracture surface of steel 348 WR to 540MPa YS in simulated BWR water at 288°C.



Figure 3-23 Section through crack in 12Cr28Ni0.5Si steel in the as warm-rolled state, tested in simulated PWR primary water at 288°C



b)

Figure 3. Intergranular crack growing close to the fusion line.



Kuva 8.2.5a Kloridien aiheuttamia jännityskorroosiomurtumia ruostumatonta terästä SS 2343 olevassa lauhdeputkessa. Lauhdeputken lämpöeristeeseen oli päässyt klorideja sisältävää vettä, mikä aiheutti noin 100 °C lämpötilassa olevaan lauhdeputkeen kuvassa näkyvät vauriot.

Oy Kymmene Ab/VVT/MRG



Kuva 8.2.5b Kuvaan 8.2.5a liittyvä mikroleikkauskuva jännityskorroosiomurtumasta putken seinämässä.

VTT/MRG

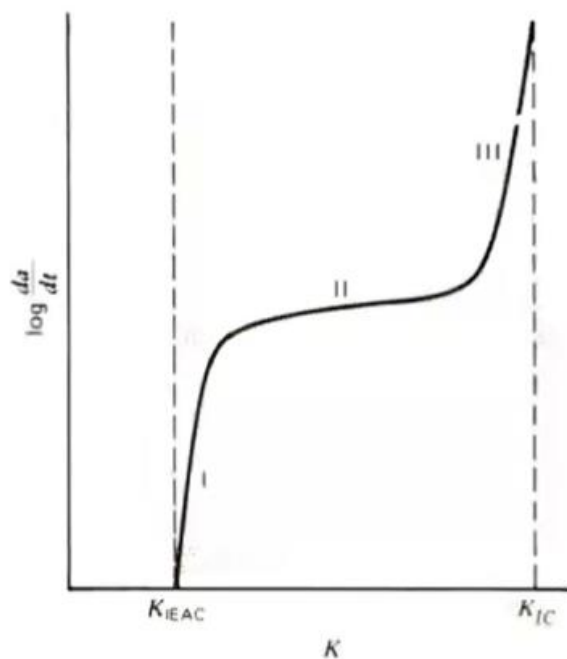


**FIGURE 11.17** Diagram showing three stages of environment-assisted cracking under sustained loading in an aggressive atmosphere. Lower and upper  $K$  limits of plot determined by  $K_{IEAC}$  and  $K_{IC}$ , respectively.

## Särönkasvunopeus

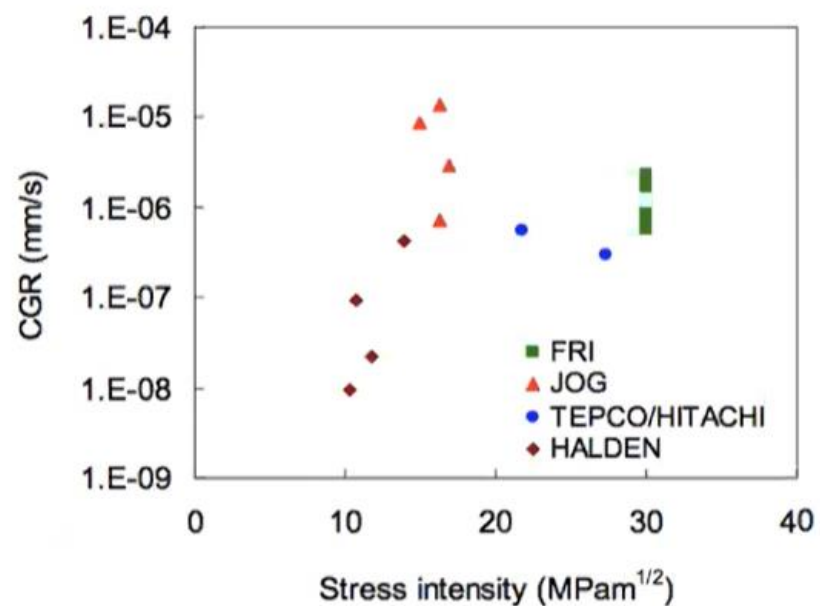
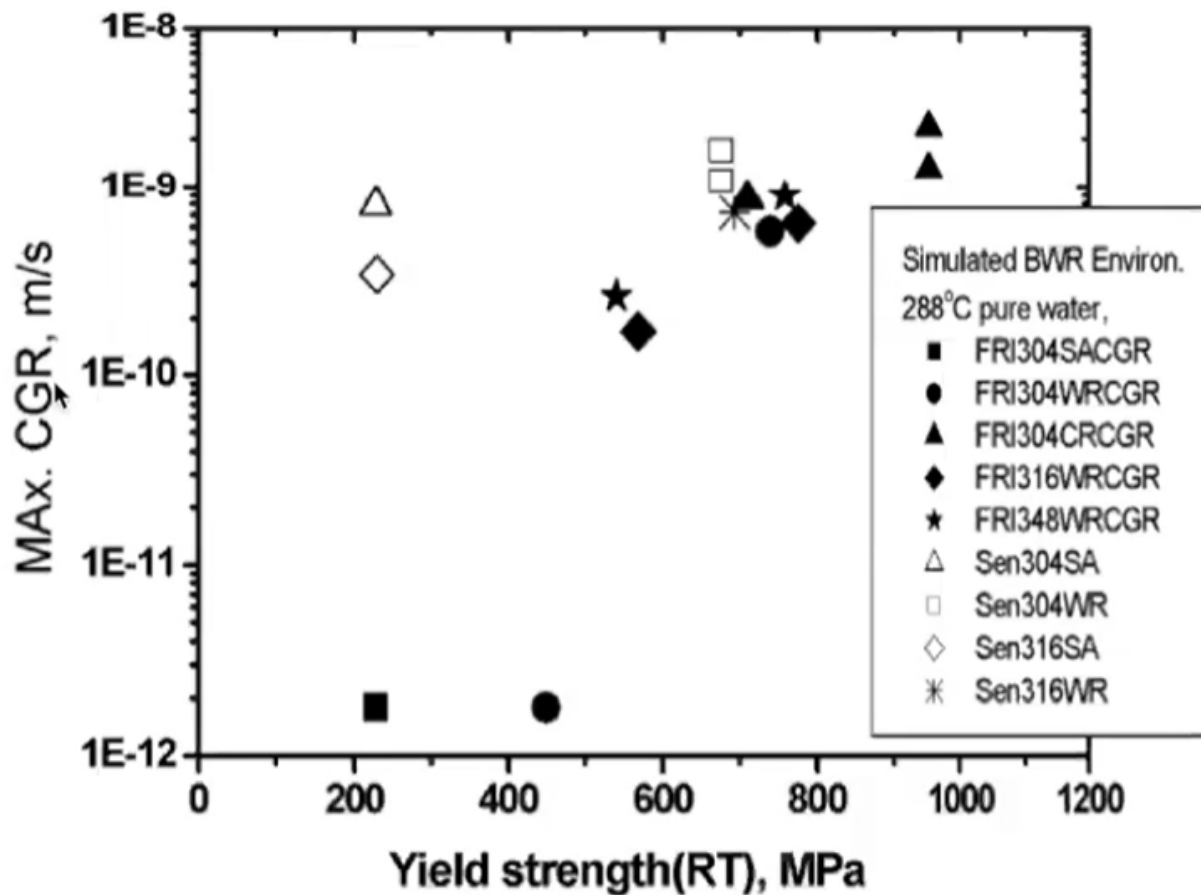


Figure 4-11. CGR vs. stress intensity level for SS 304 and 304L.



## Crack growth rate

**Difficult to predict**

- Large growth rates observed
- Large scatter

**Hardening increases susceptibility**

**Cold working increases susceptibility**

**Sensitization**

# Sensitization in stainless steels

**Long exposure near 400° C causes chromium carbide precipitation at grain boundaries**

- During welding HAZ

**Associated Cr-depleted zone**

**=> becomes susceptible to IG fracture**

**=> Ti or Nb stabilization**

- e.g. AISI 347

**=> Low carbon steels**

- e.g. AISI 304L

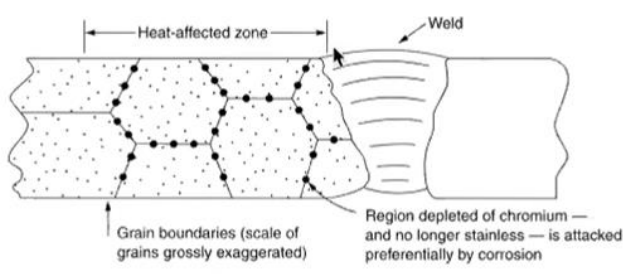
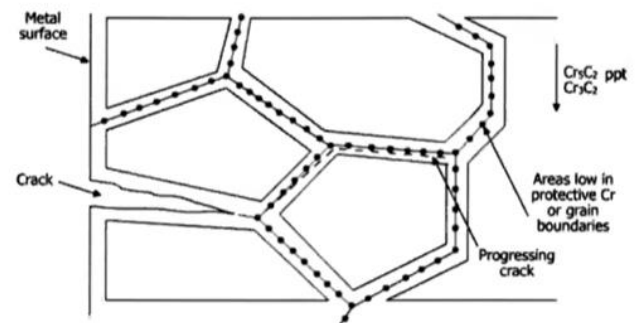
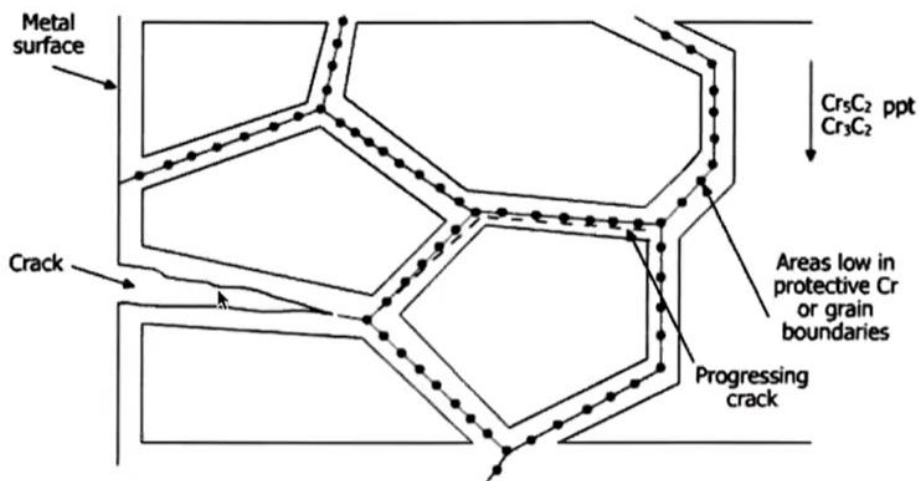


Figure 27.7 Weld decay in stainless steel.





## Stress corrosion in different metals



Kuva 8.2.5c Ammoniakkipitoisen kostean ilman aiheuttama jännityskorroosiomurtuma (season cracking) messinkisen spriikeittimen säiliön vaipassa. Säiliön vaippaan on jäänyt valmistuksesta jäännösjännityksiä, jotka ovat aiheuttaneet esitetyssä korroosioympäristössä kuvassa näkyvän murtuman.

Esselte Studium/Korrosionsinstitutet



Figure 3-55 Season cracking of German ammunition.

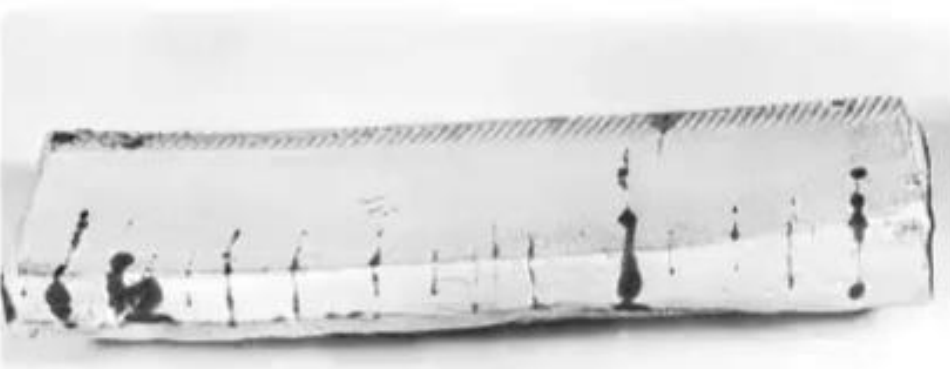


Figure 3-56 Carbon steel plate from a caustic storage tank failed by caustic embrittlement.  
*(Imperial Oil, Limited, Ontario, Canada)*



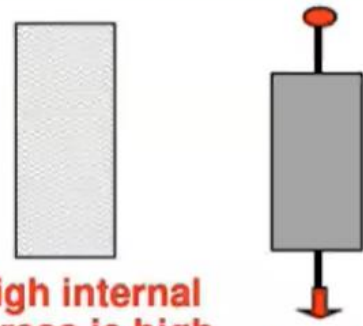
**Figure 16.1** Steam drum bolt that failed by caustic stress-corrosion cracking. Note the typical brittle character of the fracture. (*Courtesy of National Association of Corrosion Engineers.*)

## Stress corrosion in Al

### Stress corrosion.

Stress corrosion occurs in some susceptible aluminium alloys † in certain conditions of stress (internal and/or external) combined with certain microstructures coupled with exposure to a corrodng environment eg salt water.

† eg Al-Cu, Al-Mg, Al-Zn-Mg



High internal  
stress ie high  
level of cold  
work

# Susceptibility

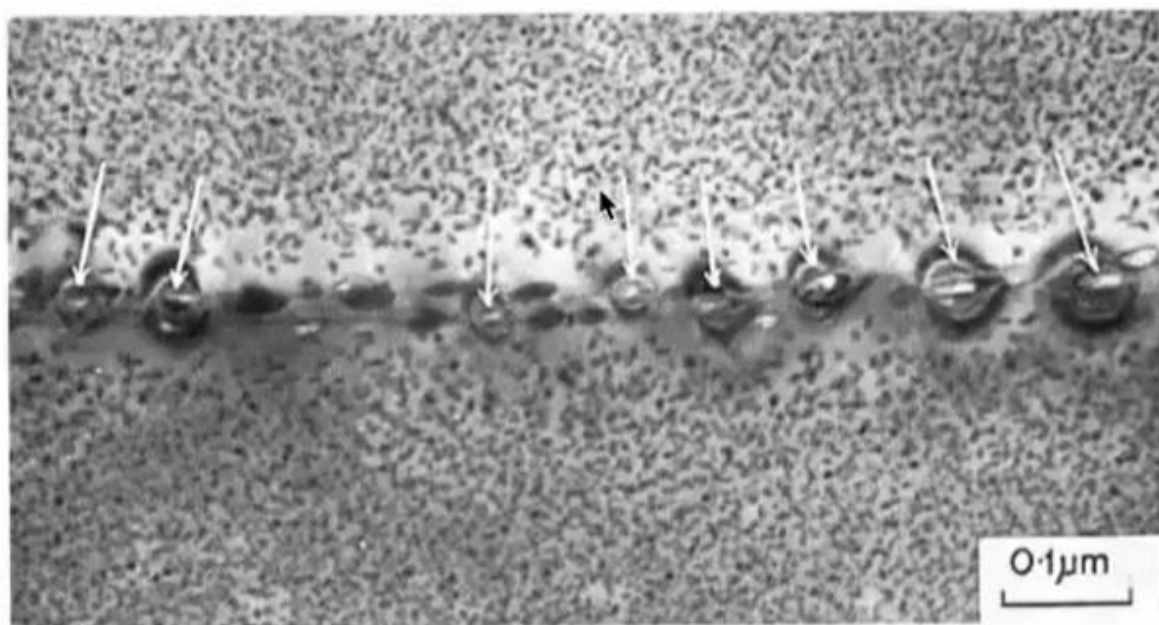
**Composition (Al-Cu, Al-Mg, Al-Zn-Mg)**

## Structure

- PFZ – anodic zone
- GP zones – susceptible
- grain boundary precipitates
- concentration differences near grain boundaries
- hydrogen diffusion in grain boundaries → hydrogen embrittlement

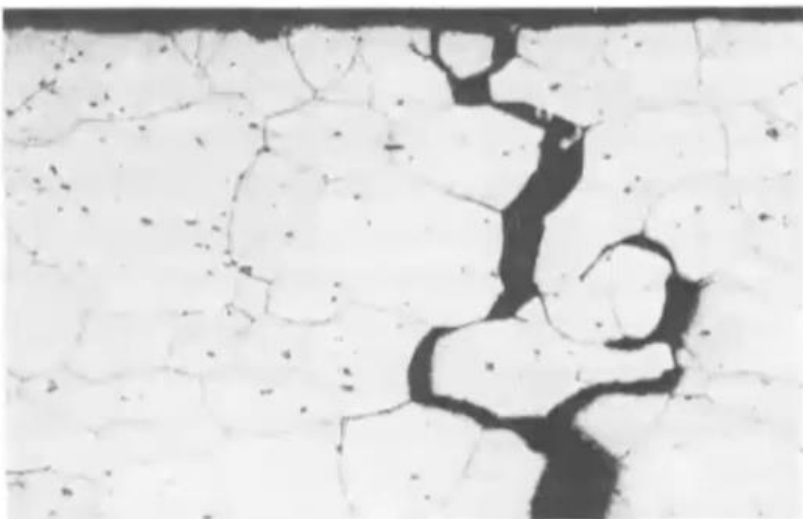
## Stress

## Environment



**Fig. 2.33** Transmission electron micrograph showing hydrogen bubble development at precipitate particles in a grain boundary of a thin foil of an artificially aged Al-Zn-Mg alloy exposed to laboratory air for three months (from Scamans, G. M., *J. Mater. Sci.*, 13, 27, 1978)

Figure 173: Intergranular stress-corrosion crack on the surface of an extrusion of AlZnMg1 alloy. The structure is recrystallized, which favors development of stress-corrosion cracking.



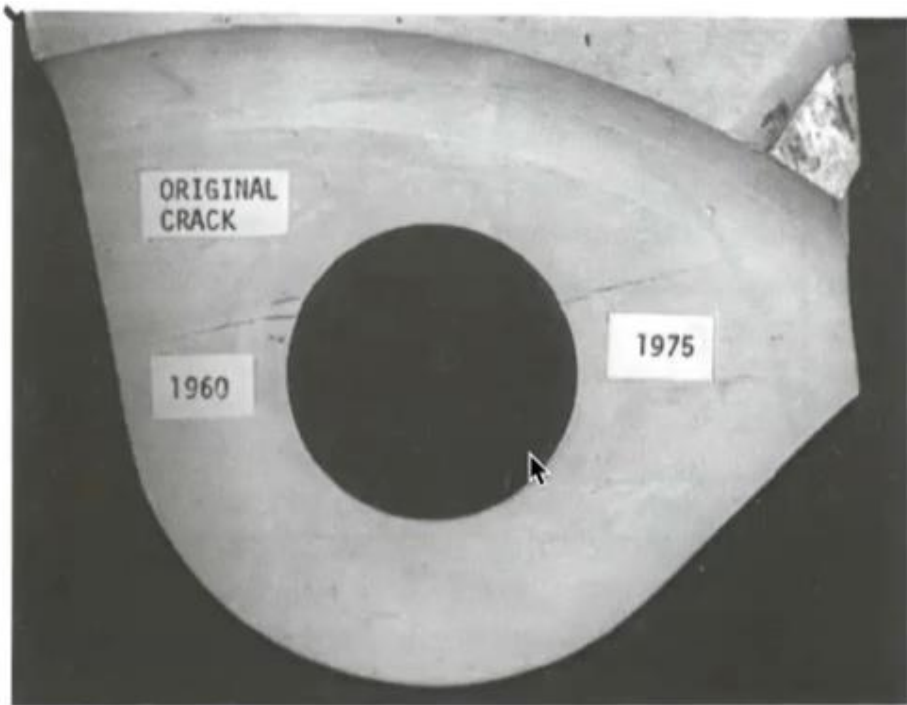
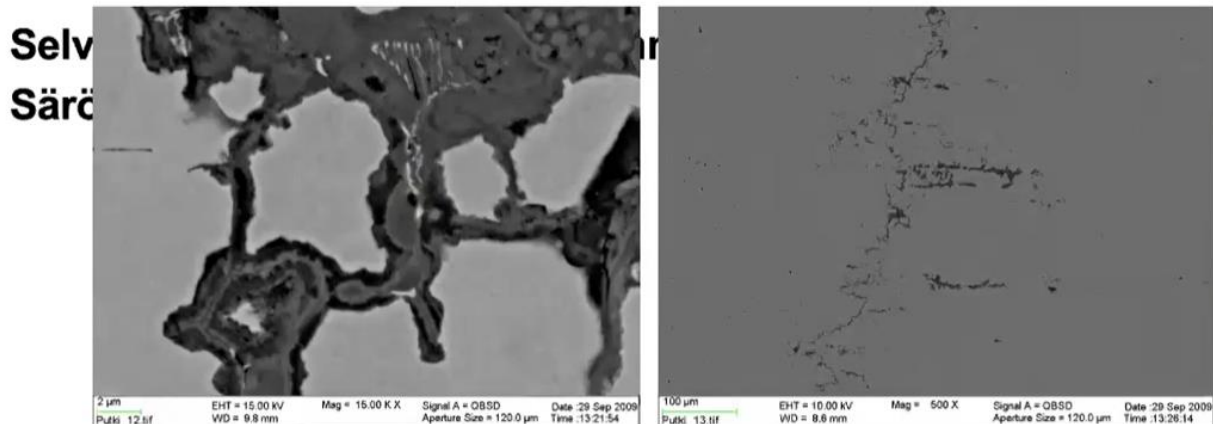


Fig. 3.28 Stress-corrosion cracks in a cold-water quenched Al–Zn–Mg–Cu alloy forging.

## Carbon steel SCC in Ethanol



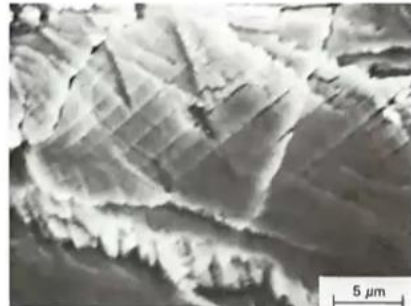
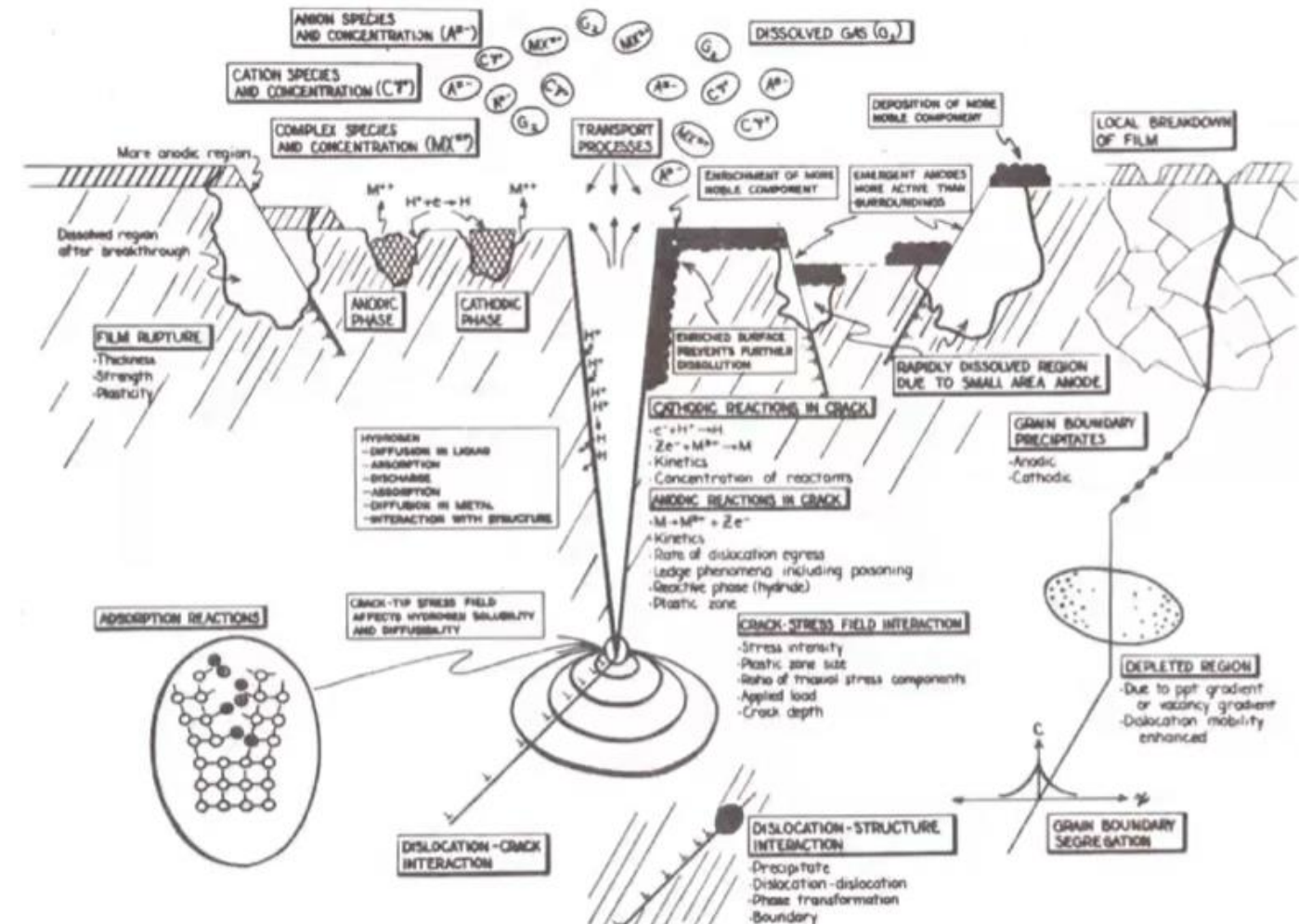


FIGURE 11.8 Transgranular stress corrosion cracking fracture surface in type 310S stainless steel. Fracture bands were produced in load pulse (10-s spacing) experiments and reflect a discontinuous cracking process. (From Hahn and Pugh<sup>34</sup>; copyright, American Society for Testing and Materials, 1916 Race Street, Philadelphia, PA, 19103. Reprinted with permission.)

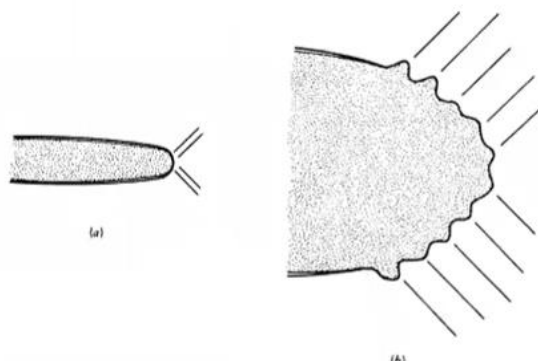


FIGURE 11.7 Diagram showing film-rupture model. Localized plastic flow at crack (a) results in numerous film-rupture events associated with transient anodic dissolution (b). (From Burstein and Pugh<sup>35</sup>; with permission from the Metallurgical Society of AIME.)

# Hydrogen cracking

## Hydrogen embrittlement

**Hydrogen in solid solution increases brittle fracture risk**

- Especially during slow strain rates

**Hydrogen can come from**

- welding (wet welding rods etc.)
- electrolytic treatments
- corrosion
- corrosion protection

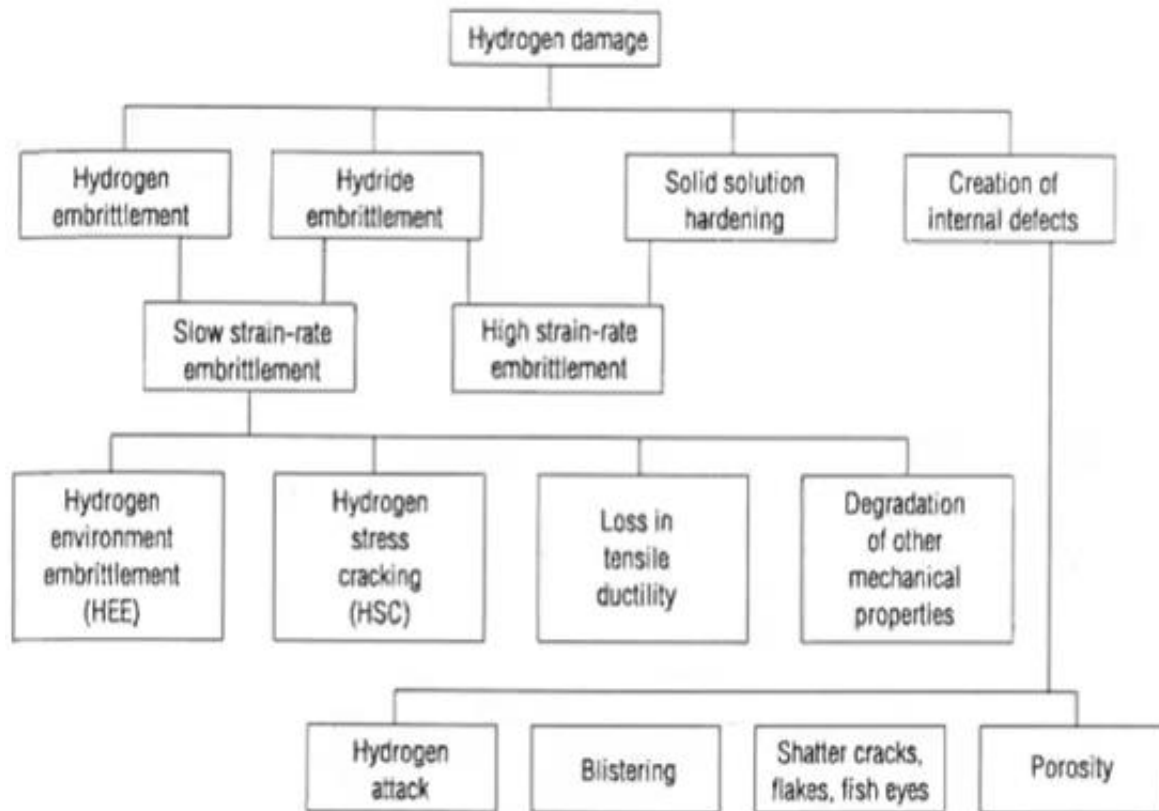


**Fig. 6.7** Various classifications of hydrogen damage<sup>25</sup>

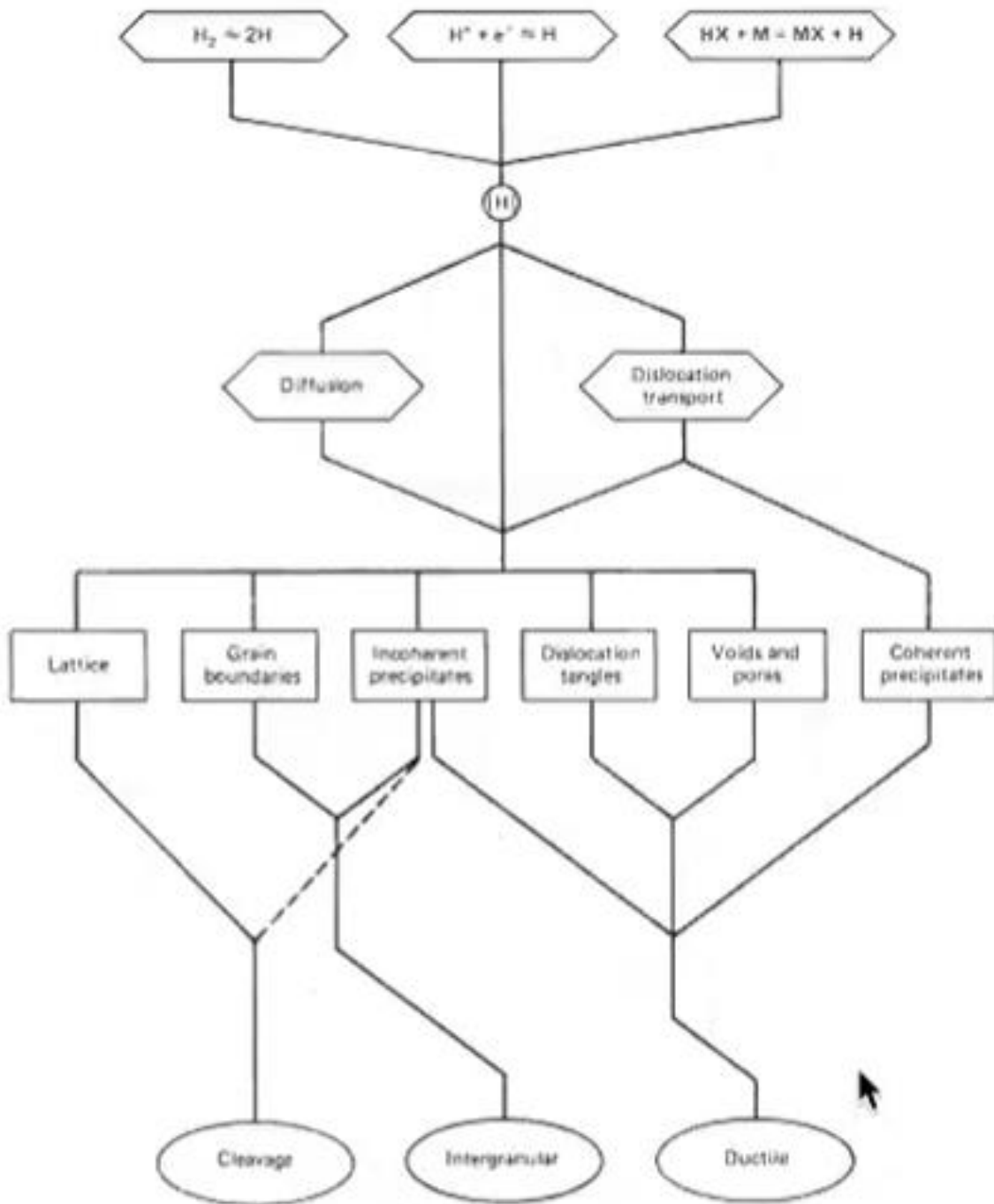
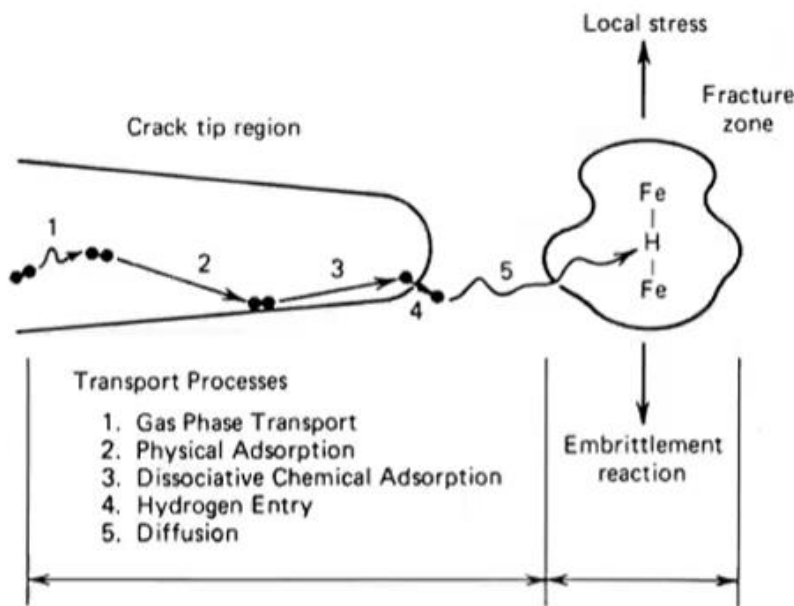
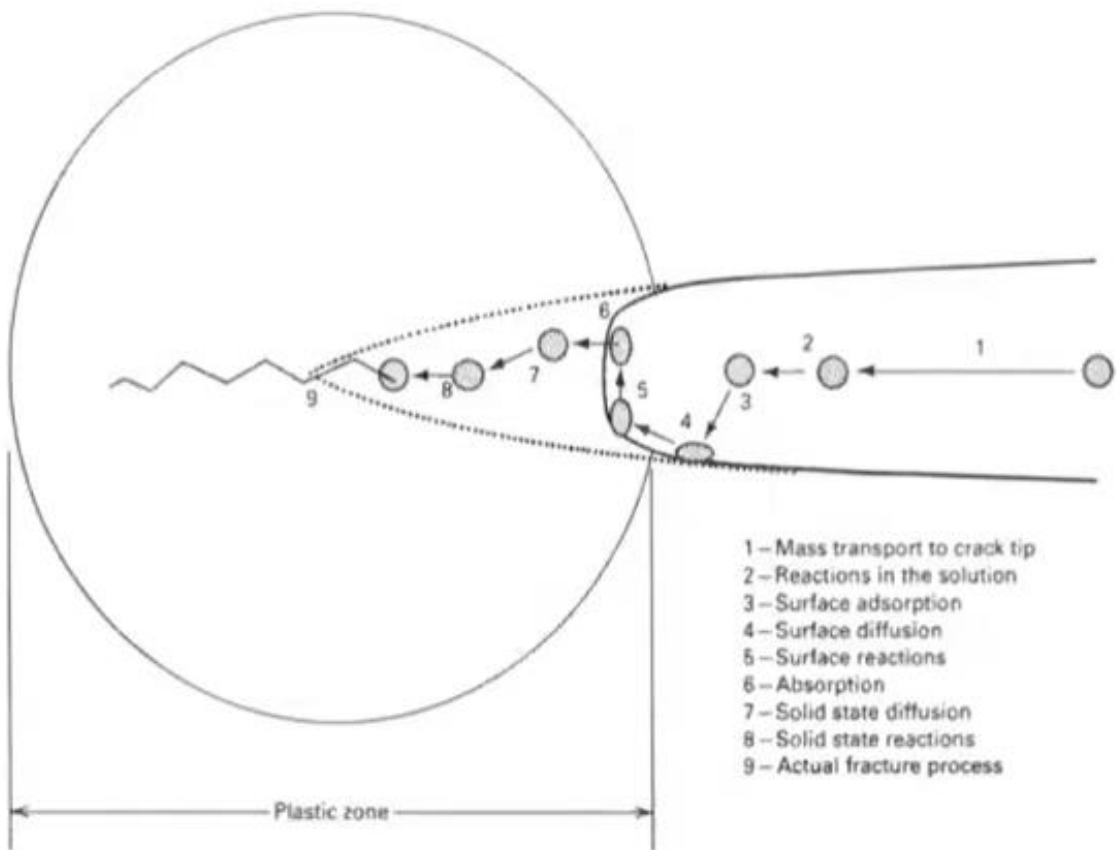
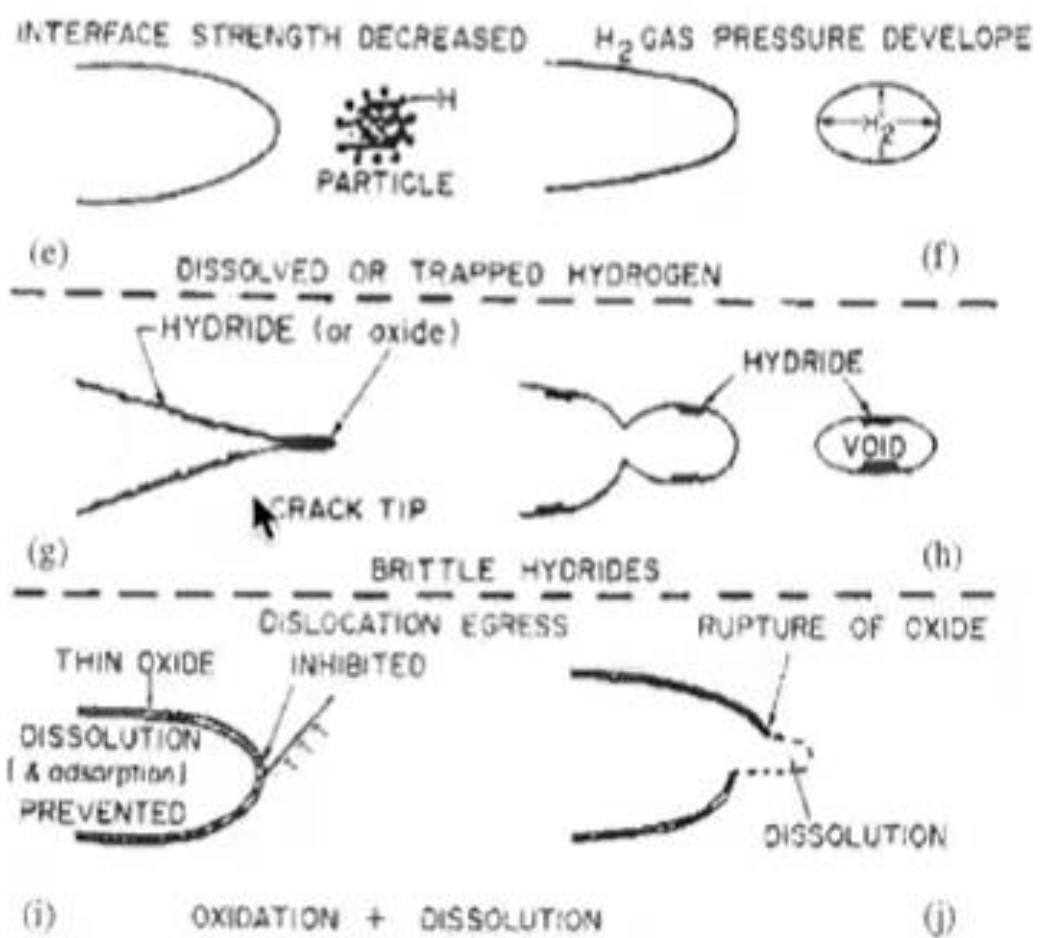
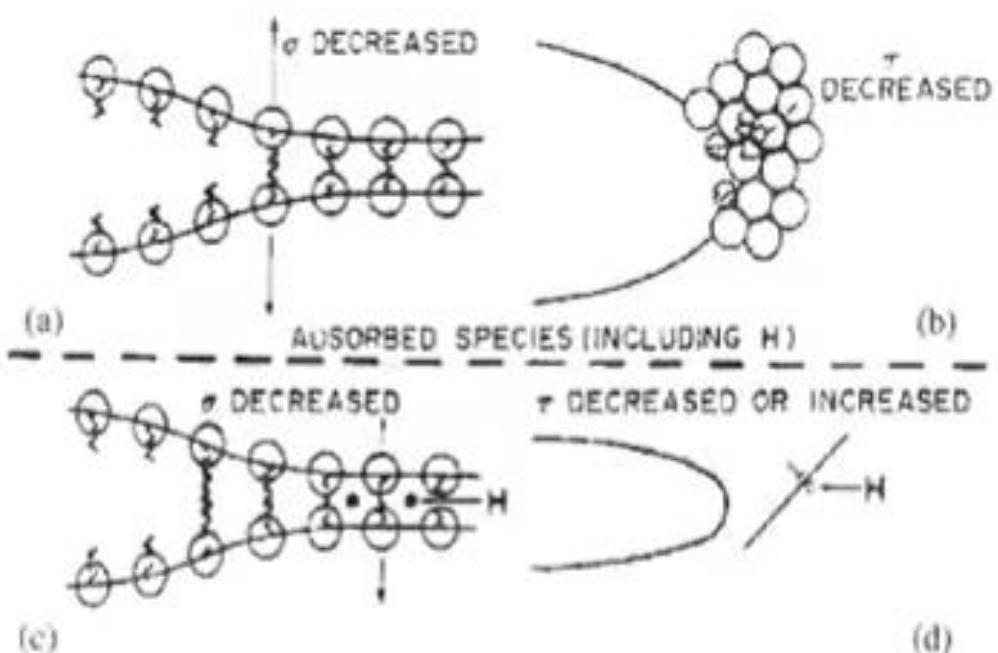


FIGURE 11.4 Flow diagram depicting hydrogen sources, transport paths, destinations, and induced fracture micromechanisms. (From A. W. Thompson and I. M. Bernstein,<sup>5</sup> *Advances in Corrosion Science and Technology*, Vol. 7, 1980, p. 145; with permission from Plenum Publishing Corporation.)



**FIGURE 11.2** Various processes involved in the hydrogen embrittlement of ferrous alloys. (From Williams et al.<sup>11</sup>, with permission from the Metallurgical Society of AIME.)





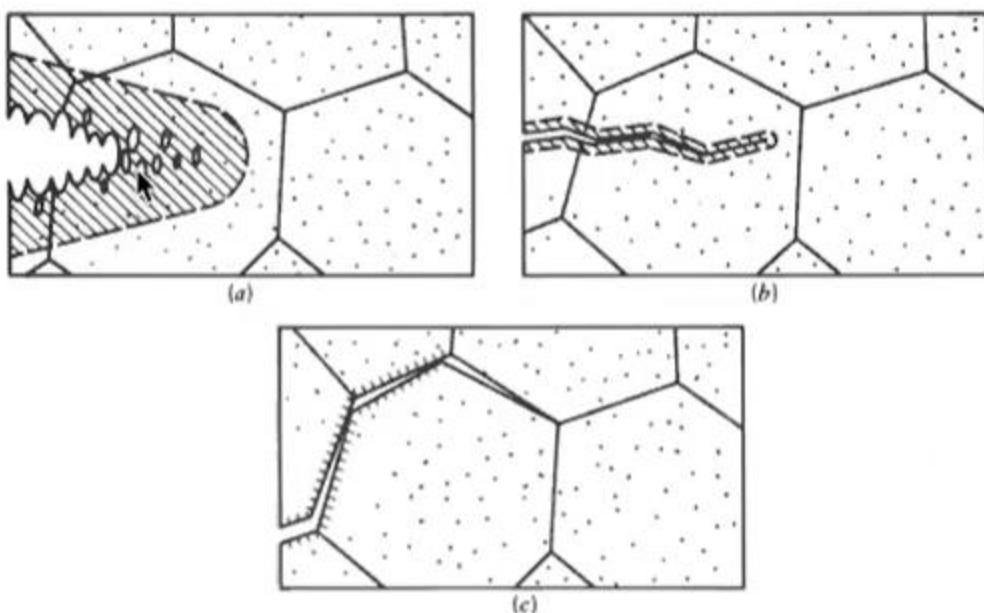


**FIGURE 11.6** Schematic representation of different hydrogen-induced fracture paths as a function of stress level. (a) High  $K$  level generates microvoid coalescence; (b) intermediate  $K$  level generates transgranular fracture by a quasicleavage mechanism; (c) low  $K$  level leads to intergranular fracture path. (From Beachem<sup>13</sup>; with permission from the Metallurgical Society of AIME.)

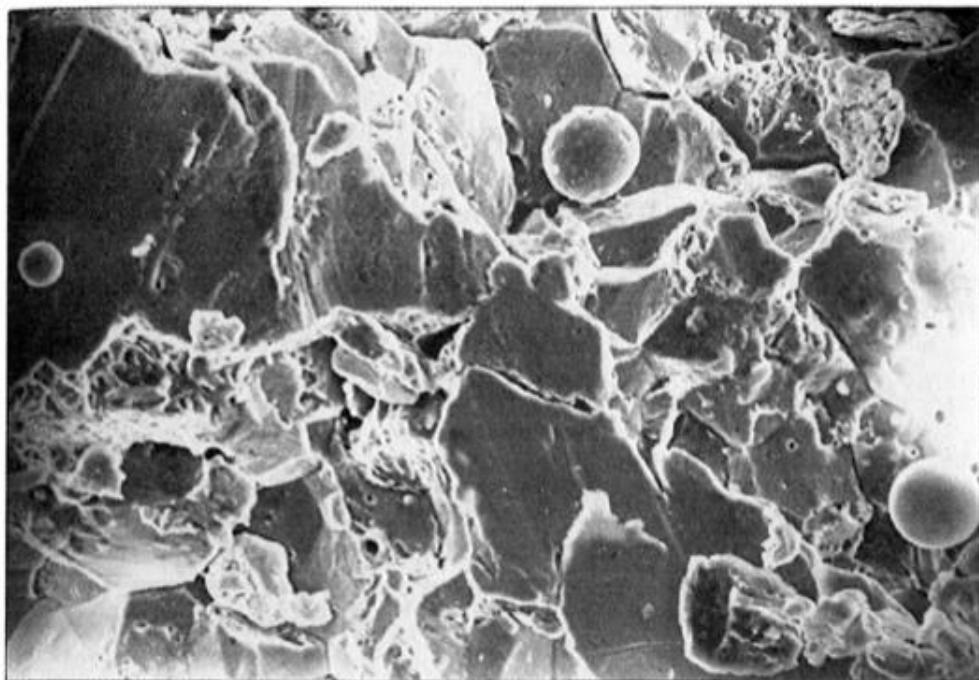


**Fig. 4.27** SEM photograph of a hydrogen embrittled fracture showing grain boundary yawning, intergranular cracking, micropore, ductile hairline crack, dimple structures and brittle facets ( $\times 450$ )

# Hydrogen attack

## Hydrogen attack

**200-540° C temperatures**

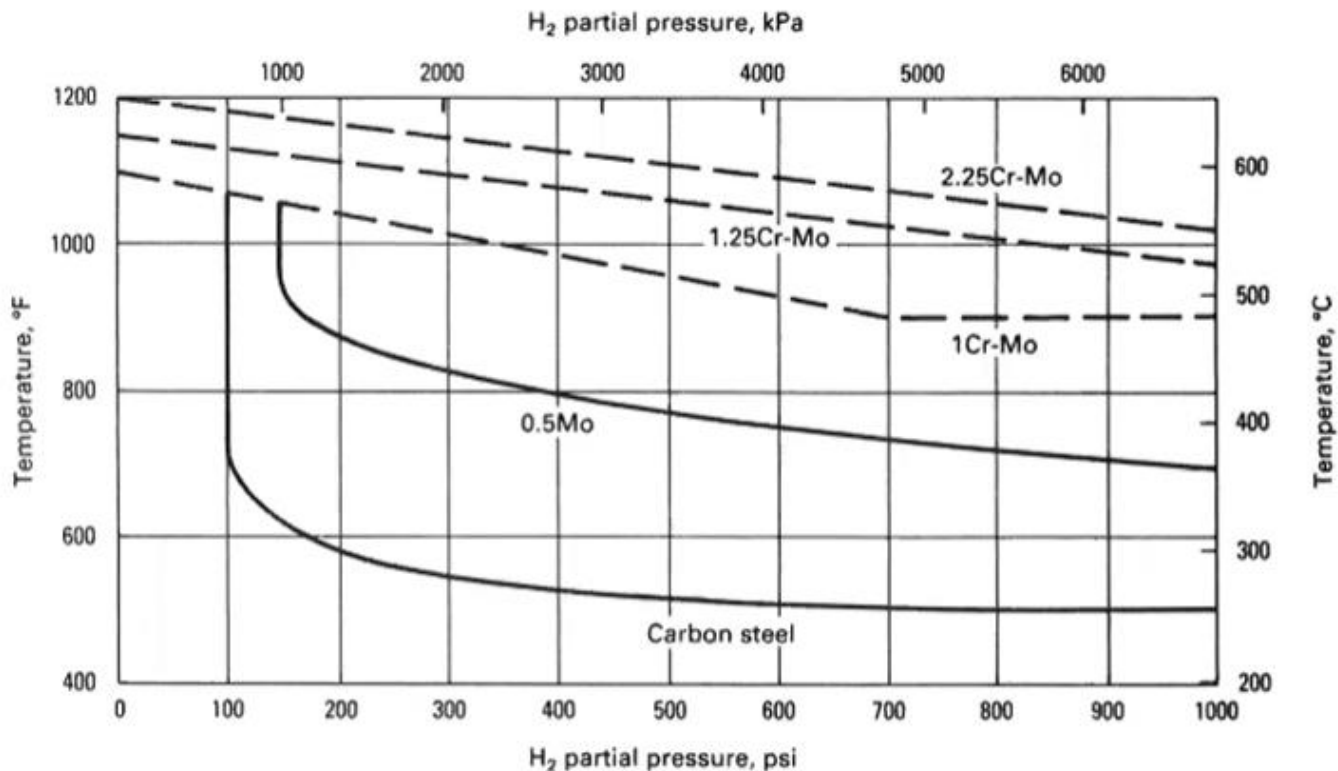
**Under high hydrogen pressure**

**Hydrogen reacts with carbon and produces methane**

**Methane forms blisters and embrittlement**

**Design with Nelson –curves**

- Safe temperatures



# Hydrogen attack

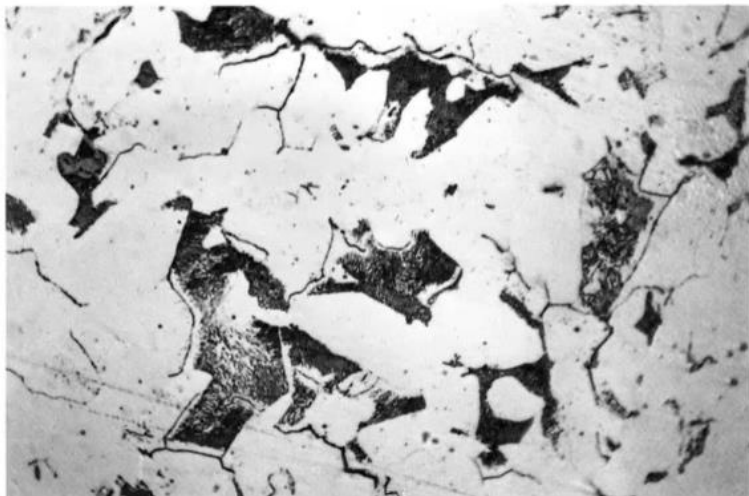


**Figure 14.1** Discontinuous intergranular microcracks resulting from methane formation in the grain boundaries. Note decarburization of adjacent pearlite colonies (dark islands). (Magnification: 500X.)

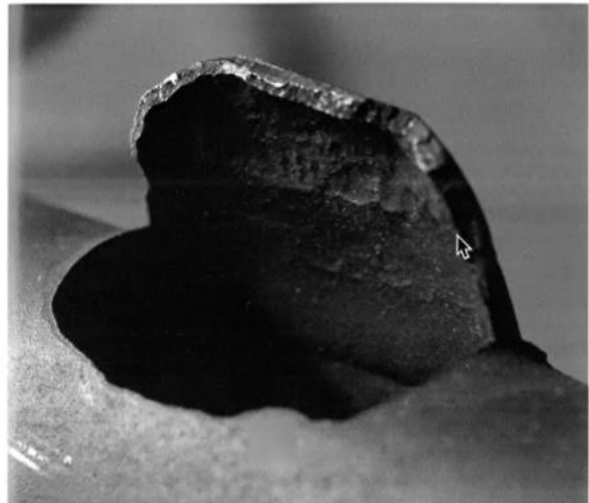


**Figure 14.2** Thick-walled burst resulting from hydrogen damage. Note areas of gouging adjacent to burst on internal surface. (Courtesy of Electric Power Research Institute.)

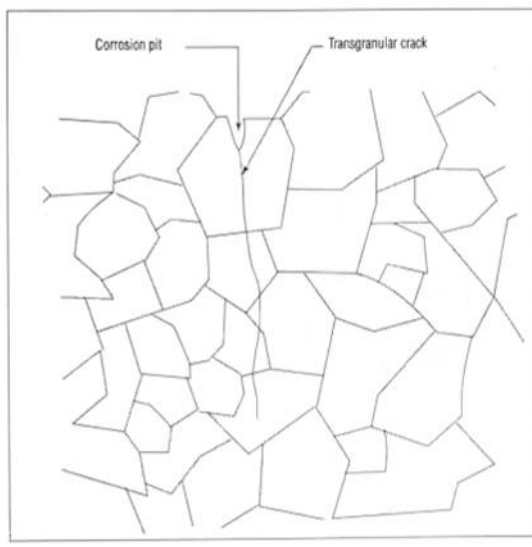
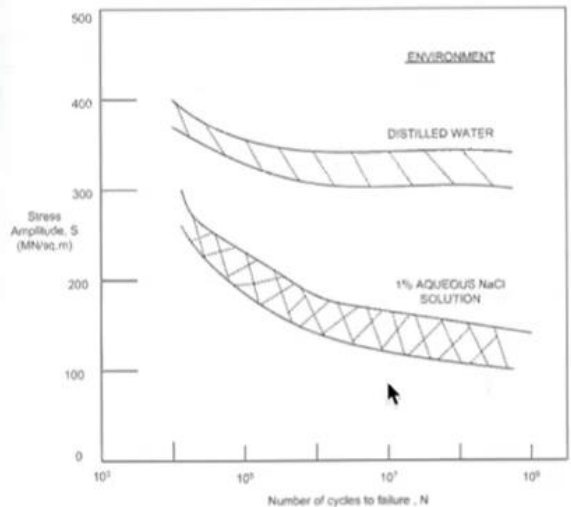
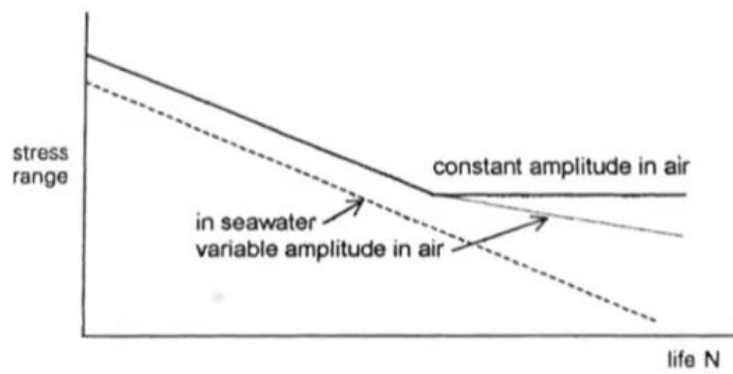
## Corrosion fatigue

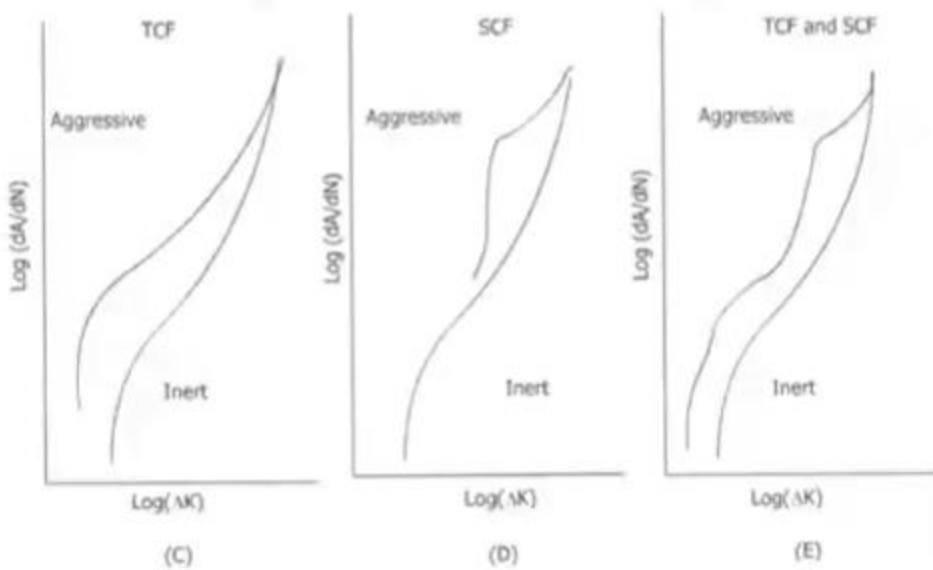
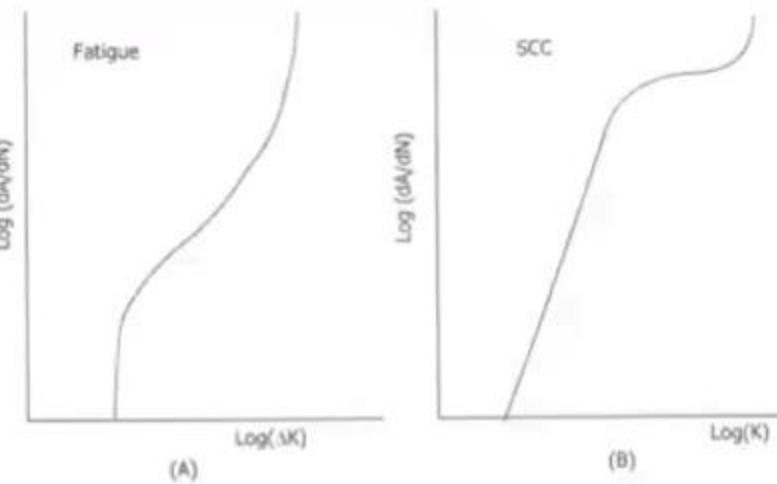
### Environmental effects

- decrease (remove) fatigue limit
- reduce fatigue life
- increase crack growth rate

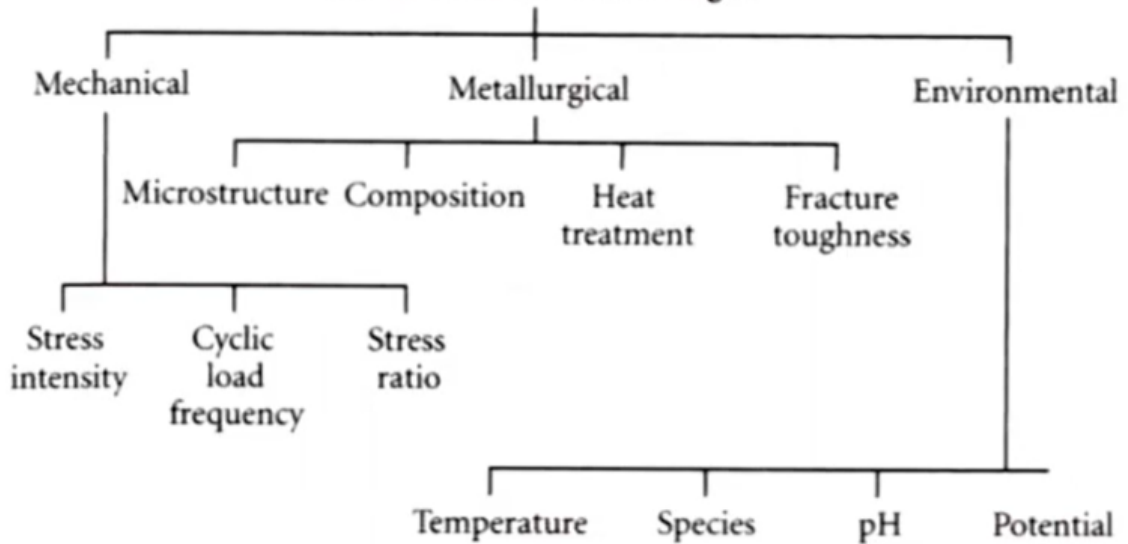
**Fatigue tests in vacuum result in higher fatigue lifes**

# Korroosioväsyminen





### Variables in Corrosion Fatigue



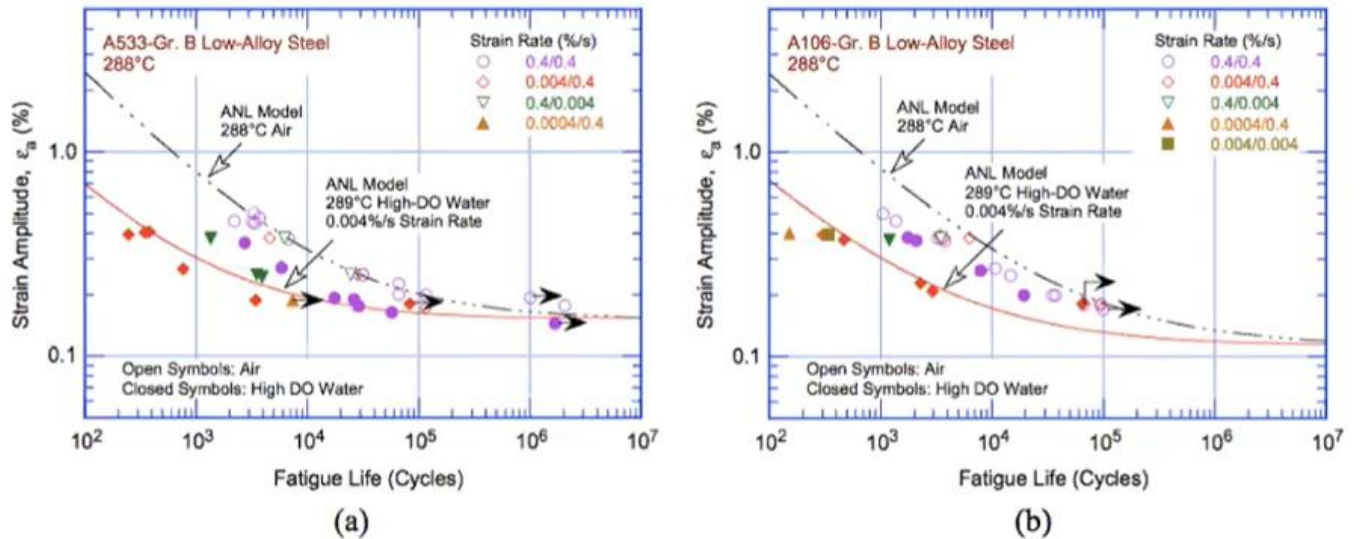
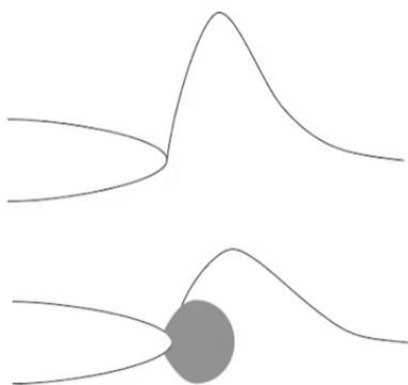


Figure 11. Strain amplitude vs. fatigue life data for (a) A533-Gr B and (b) A106-Gr B steels in air and high-dissolved-oxygen water at 288°C (Ref. 4).

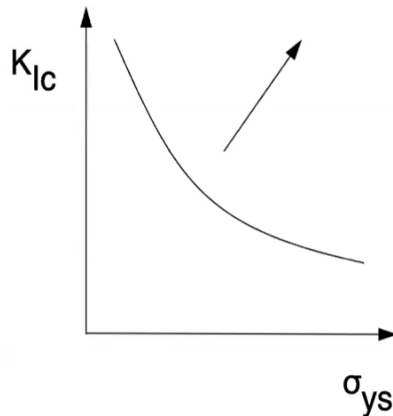
## Microstructural aspects of fracture

### Strength effect



## Strength effect

Smaller strength => higher ductility



## Nucleation

Remove initiation sites

Retard crack growth

Avoid brittle phases

Reduce inclusion size

Reduce hard, brittle inclusions

## Effect of various inclusions

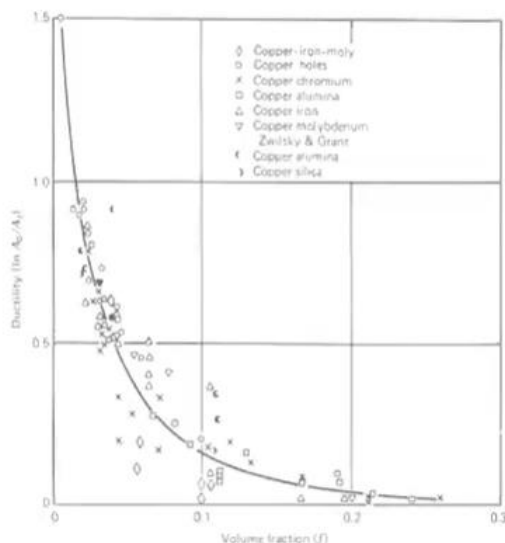


FIGURE 10.14 Effect of second-phase volume fraction on fracture ductility.<sup>19</sup> (Copyright American Society for Metals, 1962.)

# Different nucleation sites

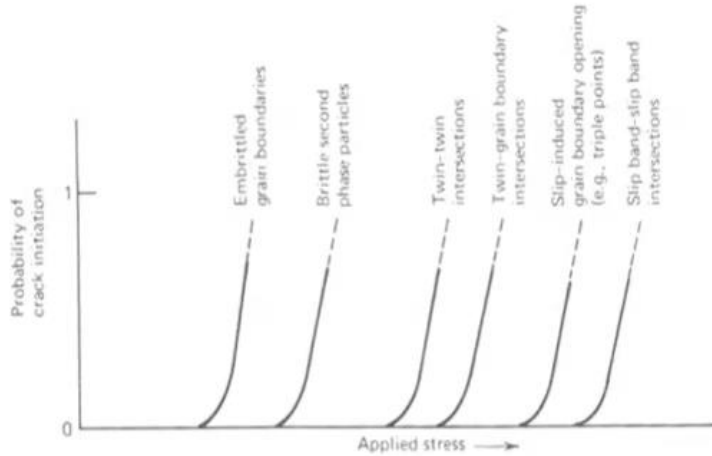
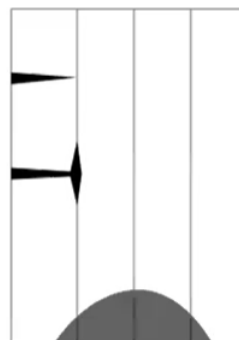


FIGURE 10.19 Probability as a function of applied stress that a particular microcrack formation mechanism will be operative.<sup>25</sup> (Reprinted with permission of Plenum Publishing Corporation, from C. J. McMahon, *Fundamental Phenomena in the Materials Sciences*, Vol. 4, 1967, p. 247.)

## Guiding or blunting cracks

Weac interfaces break and blunt crack  
Macroscopic or microscopic  
Dividers  
increase anisotropy



# Precipitation hardened alloys

## **Strength with very small precipitates**

- Maraging steels
- Various aluminium alloys

## TRIP

## **Transformation induced plasticity**

- Crack tip plasticity induces phase transformation
- Fracture energy increases

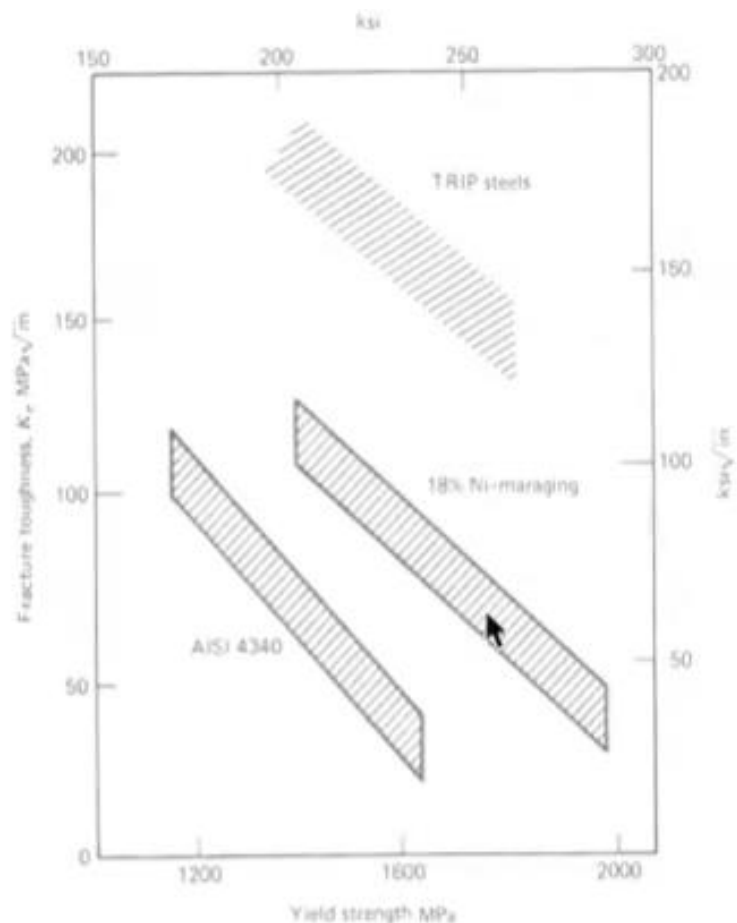
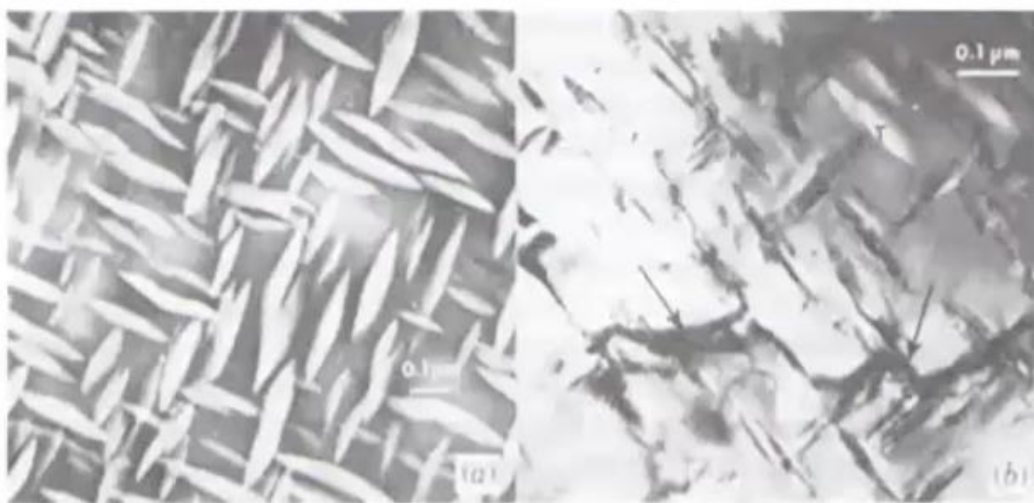


FIGURE 10.21 Fracture-toughness-tensile-strength behavior in AISI 4340, 18% Ni martensitic, and TRIP steels.<sup>20</sup> (Reprinted with permission from V. F. Zackay and Elsevier Sequoia S. A.)

## Ceramics

### Phase transformation stabilized ceramics



**FIGURE 10.30** TEM images of partially stabilized zirconia alloy, containing 8.1 mole percent  $\text{MgO}$ . (a) Coherent tetragonal  $\text{ZrO}_2$  particles embedded within a cubic  $\text{MgO}-\text{ZrO}_2$  matrix; (b)  $\text{ZrO}_2$  particles near crack plane are transformed from tetragonal to monoclinic form. Note that tetragonal particles away from crack plane are untransformed. (From Porter and Heuer,<sup>60</sup> with permission from the American Ceramic Society, Inc.)

## ABS-plastics



**FIGURE 10.34** Matrix crazes emanating from left side of rubber particle as seen on fracture surface in high-impact polystyrene. (Reprinted with permission from John Wiley & Sons, Inc.)

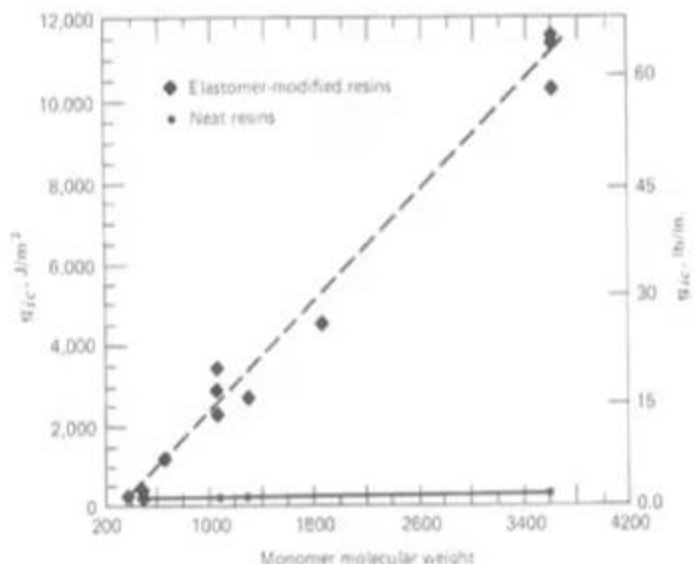


FIGURE 10.36 Fracture toughness in neat and rubber-modified epoxy resin as a function of molecular weight between cross-links.<sup>53</sup> Note dramatic improvement in composite toughness with increasing resin ductility as represented by increased  $M_w$ . (Reprinted with permission from A. F. Yee and R. A. Pearson, *Toughening in Plastics II*, 2/1 (1985), Plastics and Rubber Institute.)

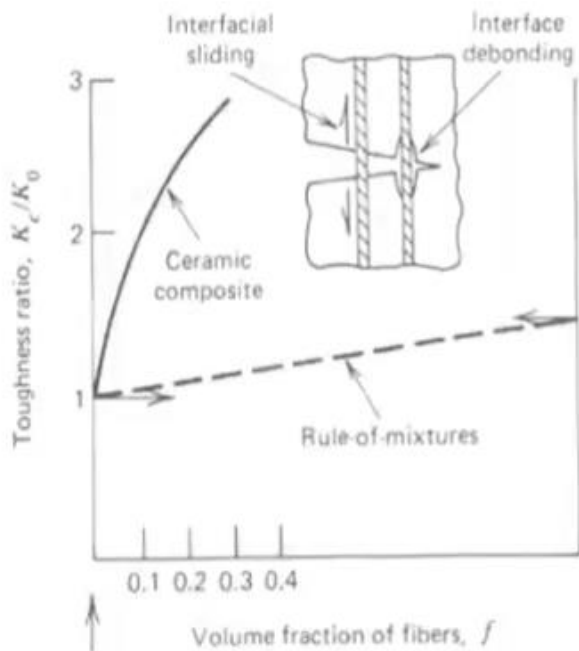


FIGURE 10.37 Relative toughness of ceramic composite as a function of fiber fraction. Toughness far exceeds that predicted from rule of mixtures.<sup>54</sup> (With permission from A. G. Evans.)

# Finer microstructural features

**Grain boundaries can stop small cracks**

**Grain boundaries cause crack deflection**

**Improves strength and ductility**

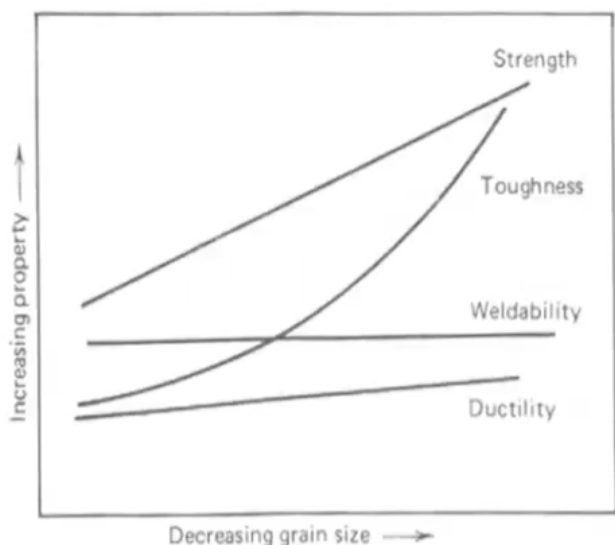


**FIGURE 10.38** Simultaneous improvement in alloy strength and toughness with decreasing grain size. Ductility and weldability are not impaired. (Reprinted with permission from American Society of Agricultural Engineers.)

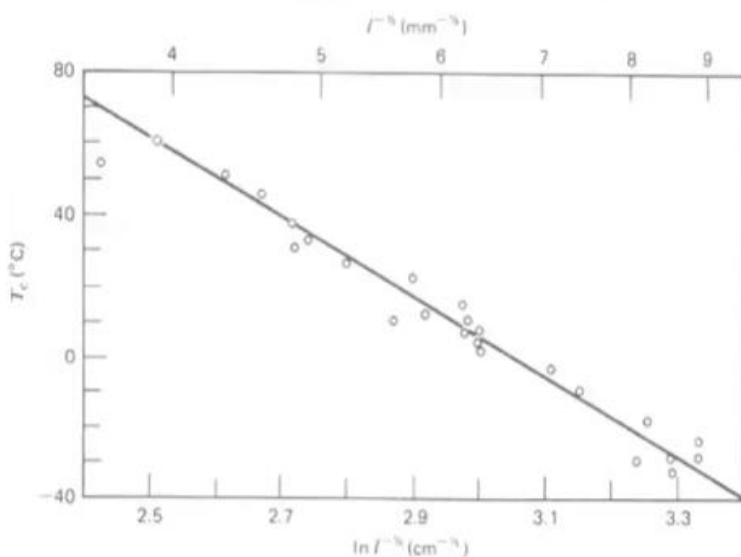


**FIGURE 10.41** Dependence of transition temperature on grain size.<sup>108</sup> (Reprinted with permission from MIT Press.)

# **Summary**

## **Ductility promoted by**

- Small round inclusions
- Fine microstructure
- Avoiding impurities

## **Embrittlement phenomena**

**Lower temper embrittlement**

**Upper temper embrittlement**

**Duplex stainless steel embrittlement**

**Hydrogen embrittlement**

## **Lower temper embrittlement**

- brittle cementite phases
- 300-400° C tempering
- fracture along former austenite grain boundaries

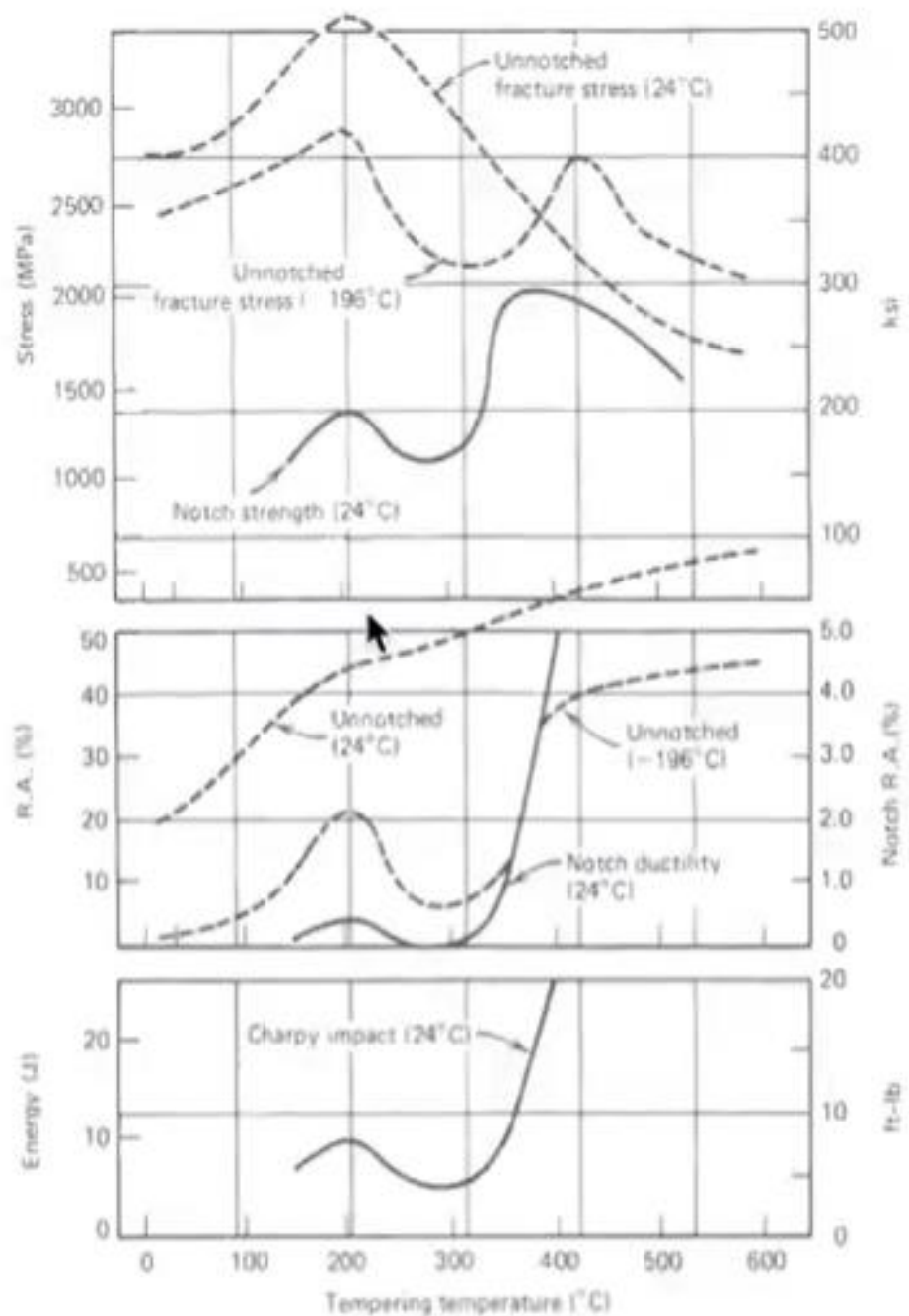


FIGURE 10.47 Notched and unnotched tensile properties at room and low temperatures for SAE 1340 steel, quenched and tempered at various temperatures. Poor properties associated with tempering in range of 300°C.<sup>12</sup> (Reprinted with permission of the American Society for Metals.)

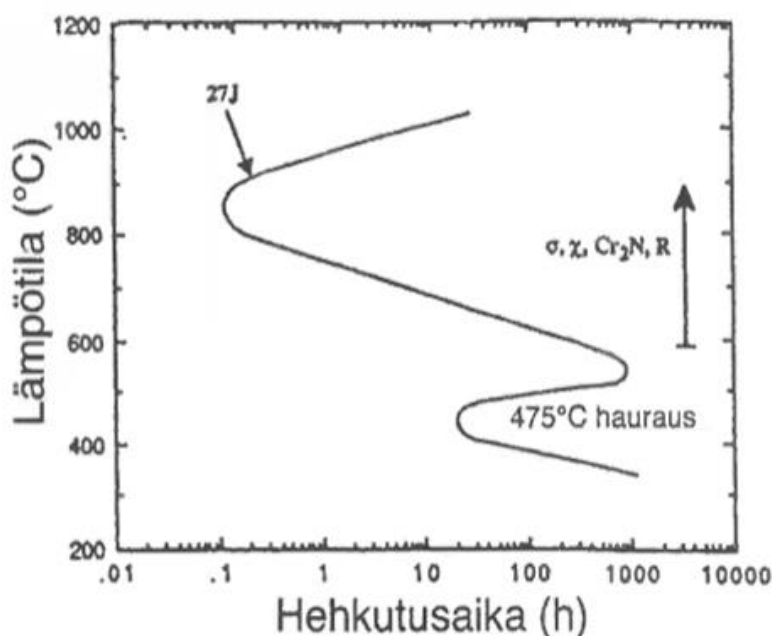
# Duplex-stainless steel embrittlement effects

Complex Fe-Cr-Ni metallurgy

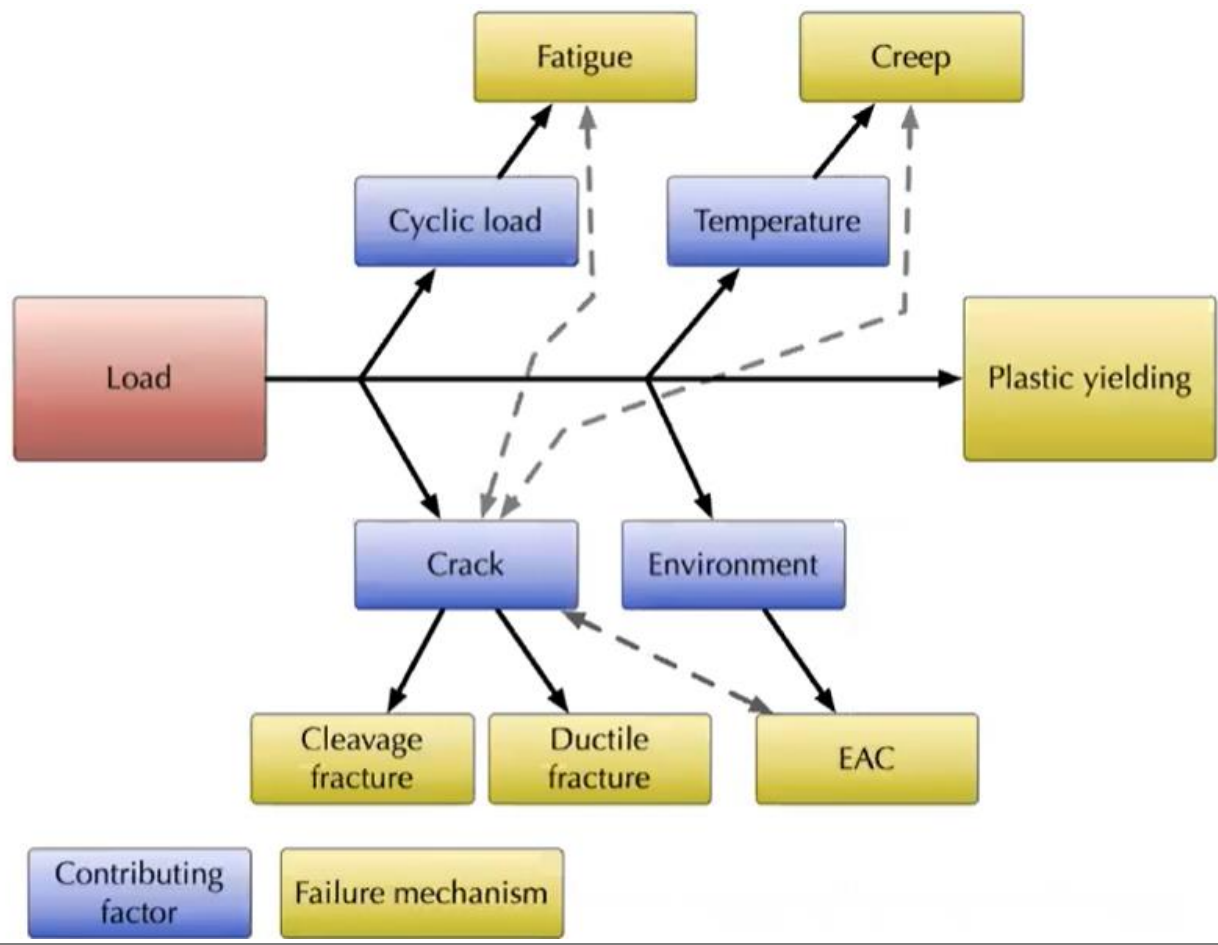
Numerous possible brittle phases

Taulukko 1. Yhteenvedo mahdollisista faaseista ruostumattomissa duplex-teräksissä. (Laitinen 1995, Nilsson 1992)

Faasi	Nimellinen koostumus	Erkautumislämpötila (°C)
$\delta$		
$\gamma$		
$\sigma$	Fe-Cr-Mo	600–1000
$\text{Cr}_2\text{N}$	$\text{Cr}_2\text{N}$	-900
$\chi$	$\text{Fe}_{36}\text{Cr}_{12}\text{Mo}_{10}$	700–850
R	Fe-Cr-Mo	550–650
$\pi$	$\text{Fe}_7\text{Mo}_{13}\text{N}_4$	550–600
$\text{M}_7\text{C}_3$	$\text{M}_7\text{C}_3$	950–1050
$\text{M}_{23}\text{C}_6$	$\text{M}_{23}\text{C}_6$	600–950
CrN	CrN	-
$\tau$		550–650
$\alpha'$		280–1000



Kuva 3. TTT-käyrä duplex-teräksissä tavattaville faaseille. (Nilsson 1992)



# Accident

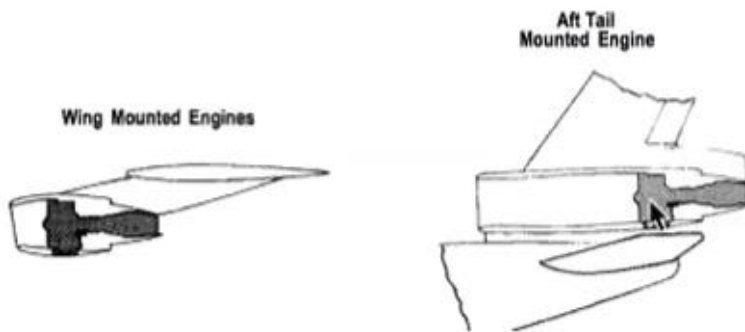
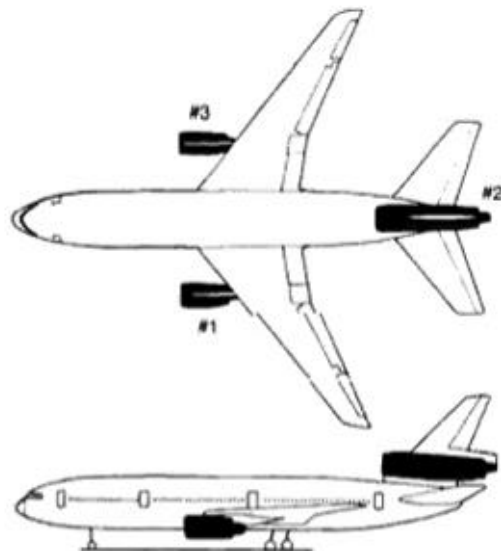
**19.7.1989 15:16 DC-10-10 (N1819) United Airlines (232)  
experienced a massive engine failure during flight**

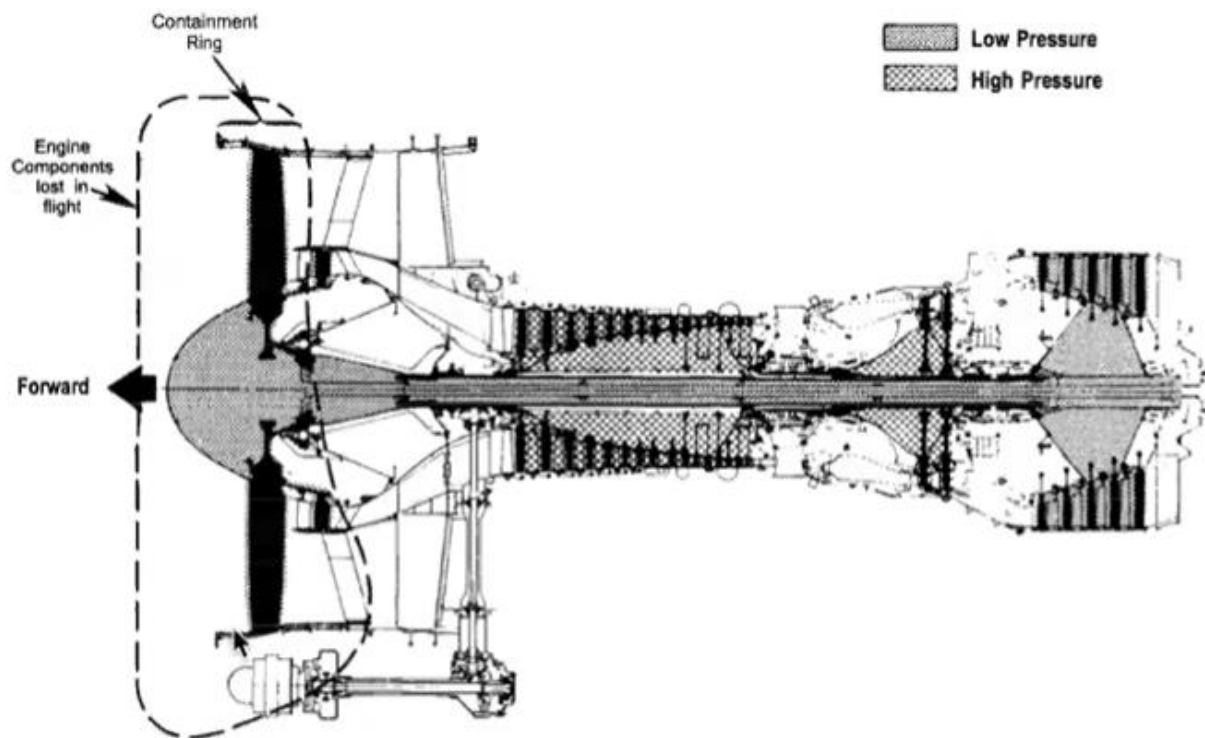
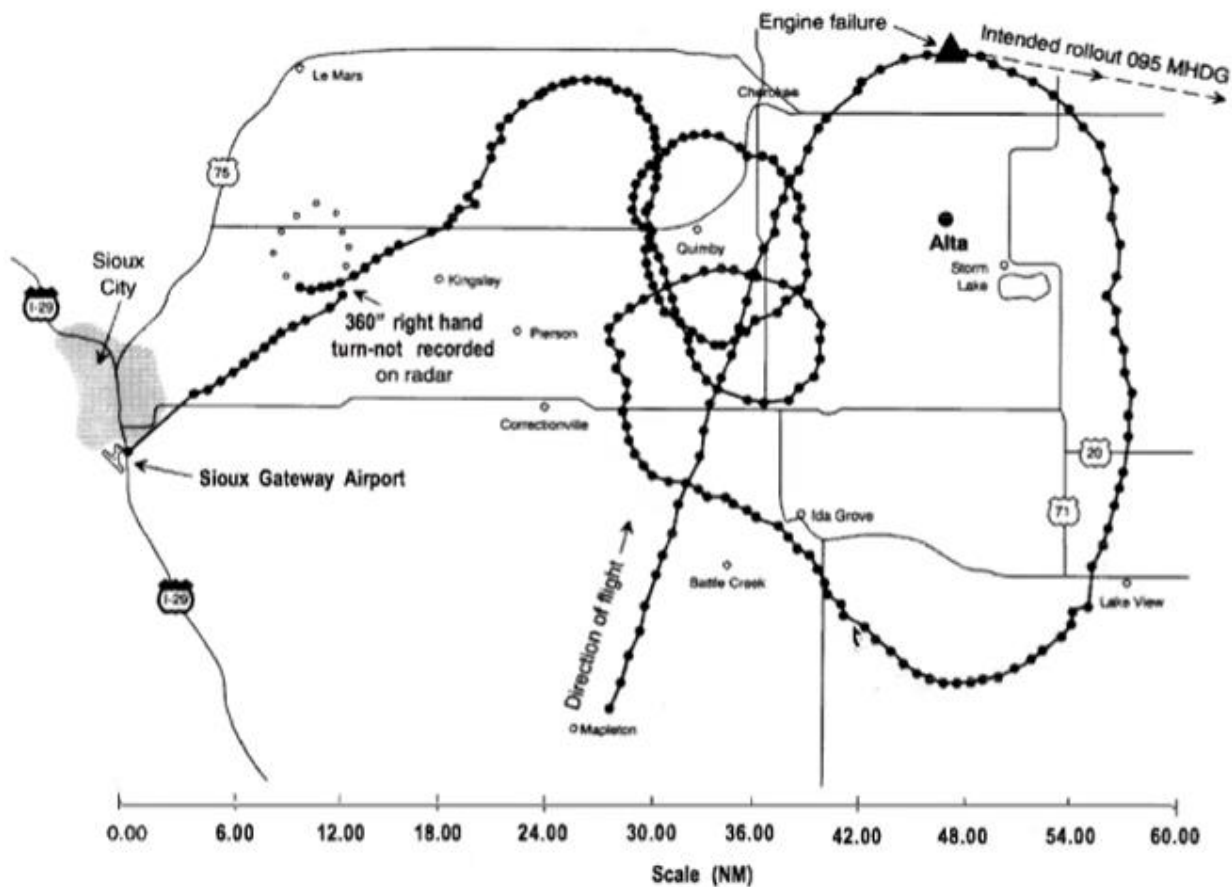
**In the airplane, a loud bang was heard. Hydraulics pressure was lost. Airplane became impossible to steer**

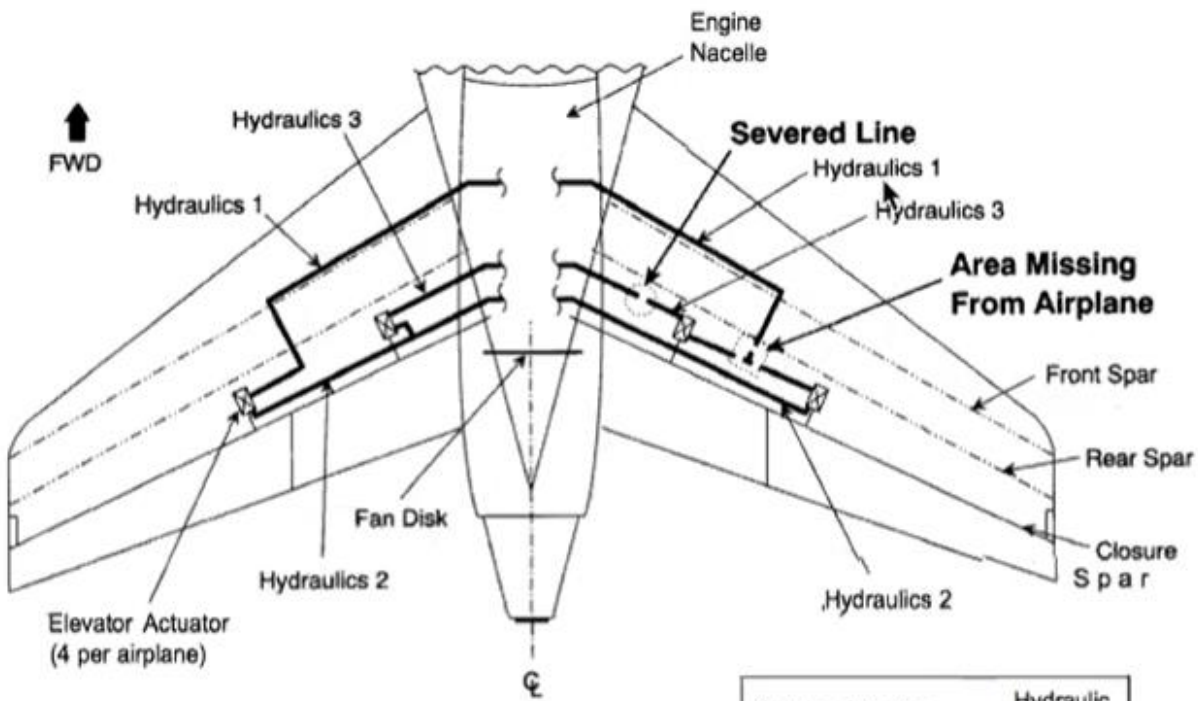
**Emergency landing was attempted to Sioux Gateway-airport**

**During emergency landing, plane hit the ground, spun around and caught fire**

**Out of 296 people on board, 111 was killed in the crash or in the following fire**

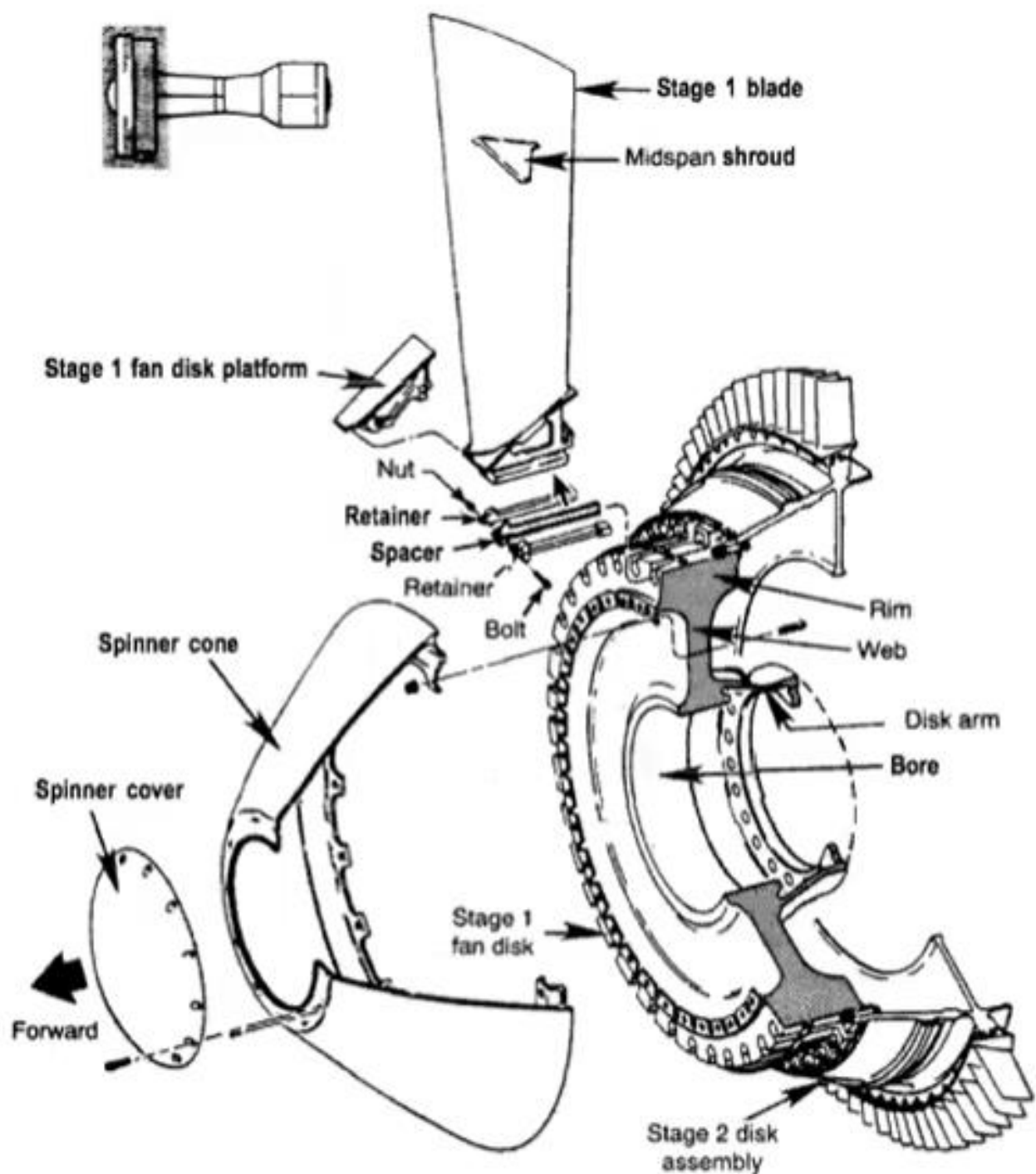






Not to Scale

Actuator Position	Hydraulic System
RH Inbd Elev	1 & 3
LH Inbd Elev	2 & 3
RH Outbd Elev	1 & 2
LH Outbd Elev	1 & 2



# Why did the fan disk break?

... and how can we prevent similar occurrences in the future?

**Primary failure "bore-to-rim"**

**Crack initiated in axle hole  
with fatigue**

**Final fracture resulted from  
fatigue crack that reached  
critical crack size**

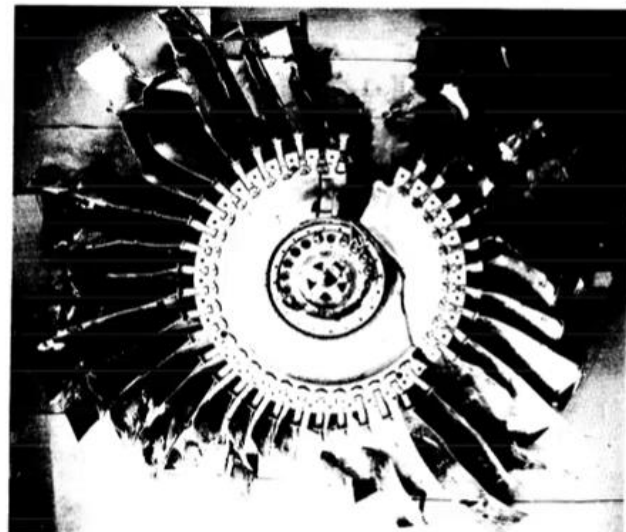


Figure 18.--No. 2 engine stage 1 fan disk (reconstructed with blades).

## Failure analysis

**Metallographic study showed crack initiation from "nitrogen-stabilized type I hard alpha defect"**

**Inclusion formed during manufacturing**

**Inclusion gone unnoticed during manufacturing inspection  
(ultrasonic, macro etching and penetrant tests)**

**At final fracture, crack size corresponds with critical size during normal operation**

**Fatigue striations showed cycle number close to engine take-off / landing cycles (15503)**

**Crack nucleation early in life (possibly first take-off)**

**Brittle inclusion broke during first full-power use and subsequently initiated fatigue crack**

**760 cycles before accident, the engine was inspected**

**Crack at 0.476" (n. 12 mm) and not detected**

## **Probable Cause**

The National Transportation Safety Board determines that the probable cause of this accident was the inadequate consideration given to human factors limitations in the inspection and quality control procedures used by United Airlines' engine overhaul facility which resulted in the failure to detect a fatigue crack originating from a previously undetected metallurgical defect located in a critical area of the stage 1 fan disk that was manufactured by General Electric Aircraft Engines. The subsequent catastrophic disintegration of the disk resulted in the liberation of debris in a pattern of distribution and with energy levels that exceeded the level of protection provided by design features of the hydraulic systems that operate the DC-10's flight controls.

## **... and how to stop from happening again**

Intensify research in the nondestructive inspection field to identify emerging technologies that can serve to simplify automate, or otherwise improve the reliability of the inspection process. Such research should encourage the development and implementation of redundant ("second set of eyes") inspection oversight for critical part inspections, such as for engine rotating components. (Class II,Priority Action) (A-90-167)